

A Hybrid Joint Moment Ratio Test for Financial Time Series*

Patrick A. Groenendijk[†]

Vrije Universiteit Amsterdam

André Lucas[‡]

Vrije Universiteit Amsterdam

Casper G. de Vries[§]

Erasmus University Rotterdam & Tinbergen Institute

SEPTEMBER 8, 1998

Abstract

We advocate the use of absolute moment ratio statistics in conjunction with standard variance ratio statistics in order to disentangle linear dependence, non-linear dependence, and leptokurtosis in financial time series. Both statistics are computed for multiple return horizons simultaneously, and the results are presented in a comprehensive way using a graphical device. We construct a formal joint testing procedure based on bootstrapped and block-bootstrapped uniform confidence intervals. The methodology is hybrid because it combines a formal testing procedure with volatility curve pattern recognition based on expert opinions. An application to forex data illustrates the procedure.

JEL Codes: C14, F31, G14

Keywords: variance ratios; absolute returns; fat-tails; linear dependence; volatility clustering; bootstrap; forex market efficiency; stable distributions.

*We thank Jón Danielsson, Laurens de Haan, Henk Hoek, and Benne Weger for helpful comments. We also benefited from a presentation at the E.S.E.M. 1998 in Berlin.

[†]Faculty of Economics, Vrije Universiteit Amsterdam, De Boelelaan 1105, NL-1081 HV Amsterdam, The Netherlands, Ph: +31-20-44-46034, Fax: +31-20-44-46005, Email: pgroenendijk@econ.vu.nl

[‡]*Corresponding author.* Faculty of Economics, Department of Finance, Vrije Universiteit Amsterdam, De Boelelaan 1105, NL-1081 HV Amsterdam, The Netherlands, Ph: +31-20-44-46039, Fax: +31-20-44-46005, Email: alucas@econ.vu.nl

[§]Faculty of Economics, Erasmus University Rotterdam, P.O. Box 1738, NL-3000 DR Rotterdam, The Netherlands, Ph: + 31-10-408-8956, Fax: +31-10-212-0551, Email: cdevries@few.eur.nl

1 Introduction

The martingale hypothesis for asset prices or weak efficiency of financial markets is one of the most intensely investigated topics in financial economics. Pagan (1996) and Campbell et al. (1997) provide excellent surveys of the relevant literature. If one augments the martingale assumption for financial asset prices with the condition that the martingale differences have constant (conditional) variance, it follows that the variance of asset returns is directly proportional to the holding period. This property has been used to construct formal testing procedures for the martingale hypothesis, known as variance ratio tests. Variance ratio tests have been applied extensively over the past decade, both in macroeconomics and finance. Examples include Campbell and Mankiw (1987) and Cochrane (1988) on output fluctuations, Fama and French (1988), Lo and MacKinlay (1988), Poterba and Summers (1988), Richardson and Stock (1989), Chow and Denning (1993), and Richardson (1993) on stock returns, and Huizinga (1987), Liu and He (1991), and Fong et al. (1997) on foreign exchange rate returns.

Variance ratio tests are especially good at detecting linear dependence in the returns, see Faust (1992). While the variance ratio statistic describes one aspect of asset returns, the idea behind this statistic can be generalized to provide a more complete characterization of asset return data. In this paper we investigate what can be learnt from using other moments in the ratio statistic besides the variance. We focus on using a combination of the variance ratio statistic and the first absolute moment ratio statistic. The first absolute moment ratio statistic by itself is useful as a measure of linear dependence if no higher order moments than the variance exist. In combination with the variance ratio statistic it can be used to disentangle linear dependence from other deviations of the standard assumption in finance of unconditionally normally distributed returns. In particular, the absolute moment ratio statistic provides information concerning the tail of the distribution and conditional heteroskedasticity. By using lower order moments of asset returns in the construction of volatility ratios, e.g., absolute returns, one relaxes the conditions on the number of moments that need to exist for standard asymptotic distribution theory to apply. We formally prove that our general testing methodology can in principle even be applied for return distributions that lie in the domain of attraction of a stable law (which includes the normal distribution as a special case). Stable laws, apart from the normal distribution, have infinite variance, such that our approach is applicable outside the finite-variance paradigm, see McCulloch (1997) for the relevance of stable variates in finance. Since in empirical work there often exists considerable controversy about the precise nature of the asset return

distribution, devising a test procedure that is valid for both finite-variance processes and infinite variance alternatives is useful for detecting linear dependence in asset returns.

If the variance is bounded, the first absolute moment ratio statistic in conjunction with the variance ratio is informative about two important data features: (i) tail thickness, and (ii) volatility clustering. First, the statistic can reveal whether the unconditional distribution of the return innovations is non-normal. The empirical evidence suggests, see Pagan (1996), that second moments appear to be finite, while moments higher than approximately the fourth or fifth are unbounded. Two properties may be responsible for this heavy tail feature, namely, conditional fat-tailedness of asset returns and volatility clustering, i.e., even with marginal thin-tailed innovations the unconditional distribution can be fat-tailed such as in the case of an ARCH process with normal distributed innovations. Second, the first absolute moment ratio statistic can also signal the presence of volatility clusters. The volatility clustering is signalled regardless whether it is of the GARCH-type, or whether it is generated by a bivariate driving process of the stochastic volatility kind. Note that the unconditional distribution of a stochastic volatility process may have all moments bounded, while this is not the case for the GARCH class processes. Indeed, we do find that the heavy tail property of the return distribution affects the absolute moment ratio statistic differently from the volatility clustering effect. Our procedures exploit these opposing effects such that it is often possible to distinguish between both causes for deviations from normality.

To the best of our knowledge the first absolute moment ratio statistic, its properties and uses are new to the literature. The first absolute moment has been used before as a measure of volatility, see, e.g., Taylor (1986) and Granger and Ding (1995). In Müller et al. (1990) the first absolute moment is computed for different return horizons. Müller et al. observe a regularity in the absolute moment estimates which is not in line with the presumption of i.i.d. normal innovations; this regularity was labeled the scaling law. In this paper we consider the ratios of these absolute moment estimates, we obtain their statistical properties under various distributional assumptions, and we explain the observed regularity behind the ‘scaling law’. In particular, we show why the deviations observed by Müller et al. should not be carelessly interpreted as evidence against the efficient market hypothesis. Furthermore, we show that the absolute moment ratio statistics contain much more information than the scaling law. Especially, when the statistic is used in combination with the variance ratio statistic, most of the characteristic features of asset returns come to the fore.

Specifically, we advocate the simultaneous use of volatility statistics based

on first (absolute returns) and second order moments (variances). In such a way we construct a test which is not only suited to detect linear dependence in asset returns, but also fat-tailedness and non-linear dependence, e.g., volatility clustering. We analytically show why moment ratios based on absolute returns can be used to detect fat-tailedness and volatility clustering, while standard variance ratios convey no information in this respect. Discriminating between the alternative phenomena is important, since they have different implications for portfolio selection and risk management.

Throughout the paper, we rely on a convenient graphical representation of the statistics: the moment ratio *curves*. This allows us to summarize a whole range of moment ratio tests for a specific return series in a comprehensible way. The graphical representation allows for a quick assessment of the salient features of the return series under study. Such an assessment builds on the ability to recognize patterns displayed in combined moment ratio plots. This ability presupposes some expert knowledge of the researcher in interpreting these plots. In the present paper, we develop this expert knowledge for time series that display characteristics typical for economic and financial data. To facilitate the formulation of an expert opinion for a specific time series, we augment our methodology with a formal statistical testing procedure. The combination of pattern recognition, expert opinion, and formal statistical testing makes our approach a hybrid one.

The formal testing procedure we propose in this paper heavily builds on the bootstrap. By performing a non-parametric bootstrap based on the empirical returns, we construct uniform confidence intervals for the range of moment ratios considered. The confidence intervals are called uniform, as opposed to pointwise, to express that the inference procedure accounts for the fact that multiple volatility ratios based on the same data set are correlated. Chow and Denning (1993) demonstrate that pointwise confidence intervals for variance ratios do not lead to reliable inference on the joint implications of these ratios when computed over various return horizons. They solve this problem by using the Studentized Maximum Modulus (SMM) distribution, which implies that the tests for different return horizons are assumed to be perfectly uncorrelated, see also Fong et al. (1997). This results in overly conservative confidence intervals. Another drawback is that their approach does not allow for an easily tractable analytical analogue in case moment ratios other than the variance ratio are used. We improve their procedure by employing the bootstrap. Apart from constructing a confidence region for the empirical volatility ratio curves, the bootstrap also proves to be extremely useful for our hybrid testing procedure through the shape of the average bootstrap moment ratio curve. The average bootstrap curve allows us to clarify effects concerning the tail behavior of asset returns if such effects are

blurred in the empirical curve due to sampling error.

As an empirical example, we apply our generalized volatility ratio tests to two daily spot foreign exchange rate series. For the US/UK rate, we find fat-tailedness, no linear dependence and moderate ARCH effects. Thus, the martingale hypothesis cannot be rejected for this series, but the forex returns are clearly not normal. For the FF/DM rate, though, we find significant linear dependence in the returns.

The remainder of this paper is as follows. In Section 2, we develop the generalized moment ratio statistic using the theory on stable distributions. We also derive conditions under which non-normality and (non-)linear correlation patterns may be detected with the moment ratio plots. In Section 3 we then describe how to perform joint inference on the moment ratios using the bootstrap. In Section 4, we present simulation experiments that illustrate the performance of the testing procedure for various types of stochastic processes. Section 5 contains the empirical analysis, while Section 6 concludes. The Appendices present the proofs of the results in Section 2.

2 A generalized moment ratio statistic

2.1 Basic theory

The standard variance ratio test from the literature is based on the assumption of an independent and identically distributed (i.i.d.) random walk for log asset prices, see, e.g., Campbell et al. (1997, Section 2.4.3). Let p_t denote the log-price process of a financial asset and let $r_t^n \equiv p_t - p_{t-n}$ denote the n -period return at time t . Under the i.i.d. random walk hypothesis for p_t , we have that

$$r_t^n = \varepsilon_t + \dots + \varepsilon_{t-n+1}, \quad (1)$$

with ε_t a set of i.i.d. random variables with mean zero and variance $\sigma^2 < \infty$. Consequently, $E((r_t^n)^2) = n\sigma^2$, where $E(\cdot)$ denotes the expectations operator. Under the assumption of an i.i.d. random walk, the variance of asset returns is linear in the return horizon. A natural statistic to test the random walk assumption is given by

$$V_n^2 = \frac{E((r_t^n)^2)}{nE((r_t^1)^2)}, \quad (2)$$

i.e., the ratio of the variance of the n -period return to that of the one-period return, normalized by the return horizon n . Under the above assumptions,

$V_n^2 = 1$. Most authors compute V_n^2 for several values of n and test whether any of these statistics differs significantly from the hypothesized value of one. Chow and Denning (1993), and Fong et al. (1997), in contrast, use a joint testing procedure based on variance ratios for several return horizons n .

We generalize (2) by replacing the square in the numerator and denominator of V_n^2 by a general constant $0 \leq \zeta \leq 2$. Discarding for the moment the return horizon n in the denominator of (2) and taking logarithms, we obtain from the generalized version of (2)

$$\log \left(E \left(|r_t^n|^\zeta \right) \right) - \log \left(E \left(|r_t^1|^\zeta \right) \right). \quad (3)$$

For the variance ratio we have $\zeta = 2$. In that case (3) is linear in $\log(n)$ with unit slope coefficient. The linearity of (3) in the log-return horizon $\log(n)$ holds under much more general conditions, as we demonstrate in our main theorem below.

Before giving the general result, we first need to focus on the class of symmetric stable distributions.¹ Let the distribution of ε_t be equal to $S_\alpha(c)$, where S_α denotes a symmetric stable law with index of stability $\alpha \in (0, 2]$, and where $c > 0$ is the scale parameter, cf. Samorodnitsky and Taqqu (1994, p. 20). In the following we assume that $c = 1$. It follows from Definition 1.1.4 of Samorodnitsky and Taqqu (1994, p. 3) and Theorem 1 in Feller (1971, ch. VI.1) that

$$r_t^n = \sum_{i=0}^{n-1} \varepsilon_{t-i} \stackrel{d}{=} n^{1/\alpha} \varepsilon_t.$$

Consequently,

$$E \left(|r_t^n|^\zeta \right) = E \left(\left| \sum_{i=0}^{n-1} \varepsilon_{t-i} \right|^\zeta \right) = n^{\zeta/\alpha} E \left(|\varepsilon_t|^\zeta \right),$$

and hence

$$\log \left(E \left(|r_t^n|^\zeta \right) \right) - \log \left(E \left(|r_t^1|^\zeta \right) \right) = \frac{\zeta}{\alpha} \log(n). \quad (4)$$

Equation (4) clearly indicates that for the class of stable distributions the relationship between (3) and $\log(n)$ is linear. The slope of the corresponding

¹We restrict our attention to the class of symmetric stable distributions since this considerably simplifies the exposition. This implies that we assume in the sequel that the ε_t are symmetrically distributed around the origin. Stable distributions are extensively discussed in Samorodnitsky and Taqqu (1994), who provide a comprehensive treatment; see also Ibragimov and Linnik (1971, ch. 2).

linear function is equal to ζ/α . Note that for this result to be valid, it must be the case that $E(|\varepsilon_t|^\zeta) < \infty$, which implies that necessarily $0 < \zeta < \alpha$ for $\alpha < 2$, and $\zeta < \infty$ for $\alpha = 2$. As was mentioned earlier, we obtain a slope coefficient of one for the Gaussian distribution ($\alpha = 2$) and the variance related plots ($\zeta = 2$). For the expected absolute returns ($\zeta = 1$), in contrast, we obtain a line with slope coefficient $1/2$ for Gaussian ε_t .

The class of stable distributions forms the basis of our main result. This class of distributions has an attractive property. For ε_i i.i.d. random numbers, let $\{a_n\}_{i=0}^\infty$ denote a sequence of increasing numbers such that $a_n^{-1} \sum_{i=1}^n \varepsilon_i$ has a nondegenerate limiting distribution. Then this limiting distribution must belong to the class of stable distributions, see Ibragimov and Linnik (1971, p. 37), and the distribution of ε_i is said to belong to the domain of attraction of a stable law. Stable distributions thus play a key role in limiting distribution theory. We exploit this phenomenon in the proof of our main theorem.

Theorem 1 *Let $\{\varepsilon_t\}_{t=1}^\infty$ denote a sequence of i.i.d. random variables with common distribution function $F(\cdot)$. Let $F(\cdot)$ belong to the domain of attraction of a stable law with index α . Let ζ be such that $0 \leq \zeta < \alpha$ for $\alpha < 2$, and $0 \leq \zeta \leq 2$ for $\alpha = 2$. Then*

$$\lim_{n \rightarrow \infty} \frac{\log \left(E \left(|r_t^n|^\zeta \right) / E \left(|r_t^1|^\zeta \right) \right)}{\log(n)} = \zeta/\alpha.$$

The proof of this Theorem is given in Appendix A. The condition that $F(\cdot)$ lies in the domain of attraction of a stable law in effect implies that there exists a sequence of constants a_n of the form mentioned above, such that the partial sums $a_n^{-1} \sum_{i=1}^n \varepsilon_i$ converge in distribution to a nondegenerate stable distribution with index α . For $\alpha = 2$, it suffices that $E(\varepsilon_i^2) < \infty$. For $\alpha < 2$, necessary and sufficient conditions for this requirement to hold can be found in Ibragimov and Linnik (1971, Theorem 2.6.1). In that case, the tails of $F(\cdot)$ need to decline algebraically, so that their shape is of the Pareto form $x^{-\alpha}$ for large values of x .

Theorem 1 shows that the relationship between (3) and $\log(n)$ is asymptotically linear with slope coefficient ζ/α . This holds for a wide class of distributions. Therefore, our testing procedure mainly builds on plots of the statistic

$$v_n^\zeta = \log(V_n^\zeta) \tag{5}$$

versus $\log(n)$, where

$$V_n^\zeta = \frac{E\left(|r_t^n|^\zeta\right)}{n^{\zeta/\alpha} E\left(|r_t^1|^\zeta\right)}. \quad (6)$$

We call such a plot a moment ratio curve. Throughout the remainder of this paper we focus on two alternative values of ζ , namely $\zeta = 1, 2$. If $\zeta = 2$, the moment ratio coincides with the well-known benchmark: the variance ratio. For $\zeta = 1$, moment ratios are based on absolute returns. Absolute returns have been used before as measures of volatility in the financial economics literature by, e.g., Taylor (1986), Müller et al. (1990), Ding et al. (1993), and Granger and Ding (1995). The moment ratio statistic for $\zeta = 1$ is implicit in Müller et al. (1990) as the slope of their regression curve. In the next subsections, we formalize what patterns can be expected for the volatility ratio curves with $\zeta = 1, 2$ in different settings of practical interest. This establishes the usefulness of our main result in Theorem 1.

2.2 Heavy tails and i.i.d. innovations

In this subsection we demonstrate how the moment ratio curve can be used to detect deviations from normality if the returns are i.i.d. As mentioned in the introduction, the variance ratio curve ($\zeta = 2$) on its own is of no use for this purpose. Here we demonstrate that a curve based on $\zeta = 2$ augmented with a curve based on $\zeta = 1$ can be very useful for detecting deviations from normality. First note that it follows from Theorem 1 that if the returns follow a stable distribution with parameter $\alpha < 2$, then we expect a linear volatility ratio curve for $\zeta = 1$ with slope coefficient larger than $1/2$. So for the special case of stable distributions, it is clear that the empirical absolute moment ratio curves will lie above the $\log(n)$ -axis if the curves are based on an (incorrect) finite variance assumption, since $1/\alpha > 1/2$. Also note that the volatility ratio curve in that case does not converge in probability to a fixed value. A similar result can be established for a larger class of fat-tailed distributions, even in case the finite variance assumption is correct. The result is summarized in the following theorem, which is proved in Appendix A.

Theorem 2 (Heavy tails) *Let the ε_t in (1) be i.i.d. with zero mean and finite variance, but not necessarily normally distributed. Then $v_n^2 \equiv 0$. Moreover, the volatility ratio curve based on $\zeta = 1$ lies above (below) the $\log(n)$*

axis for sufficiently large values of n , i.e., $v_n^1 > 0$ ($v_n^1 < 0$), depending on

$$\frac{E(|\varepsilon_t|)}{\sqrt{E(\varepsilon_t^2)}} < \sqrt{\frac{2}{\pi}} \quad (\text{respectively } >).$$

Remark 1 Note that ε_t with non-zero means can easily be coped with by first demeaning the one-period returns.

Theorem 2 states that i.i.d. innovations give rise to a flat volatility ratio curve with $\zeta = 2$. This is well-known in the literature and forms the basis for the class of variance ratio tests. Moreover, Theorem 2 reveals that moment ratio curves based on $\zeta = 1$ are non-constant if the one-period returns are non-normally distributed. More precisely, the returns must be non-normal and $E(|\varepsilon_t|)/\sqrt{E(\varepsilon_t^2)} \neq \sqrt{2/\pi}$. When considered simultaneously, the $\zeta = 1$ and $\zeta = 2$ plots should thus provide a signal on deviations from normality and on i.i.d.-ness of the returns. The following examples illustrate how the results of Theorems 1 and 2 can be applied in practice.

Example 1 Let the one-period returns be i.i.d. We consider four distributions: the normal, the Laplace distribution, the Student $t(3)$ distribution, and the shifted Bernoulli distribution. The shifted Bernoulli distribution places probability mass $1/2$ on $+1/2$ and $-1/2$, respectively. The normal distribution, with density $\exp(-x^2/2)/\sqrt{2\pi}$, is the benchmark. The Laplace distribution or two-tailed exponential with density $\exp(-|x|)/2$, has fatter tails than the normal, though the tails are still exponential. In contrast, the Student $t(3)$ distribution, with density $6\sqrt{3}/\pi(3+x^2)^2$, has algebraically declining tails. Finally, the tails of the Bernoulli distribution are thinner than those of the normal, as the Bernoulli has a compact support. The kurtosis is an often used measure for tail fatness (though the statistic is not unambiguous). For the benchmark normal the kurtosis is 3, the Bernoulli has kurtosis 1, the Laplace has kurtosis 3, while kurtosis for the Student $t(3)$ is infinite. By this measure the examples thus cover a wide range of possible cases. Note that because of the i.i.d. assumption, $v_n^2 \equiv 0$, see (1) and (2).

For the normal distribution, it is easy to see that $v_n^1 \equiv 0$. In contrast, it is proved in Appendix B that

$$E(|r_t^n|) = \frac{2\Gamma(n+1/2)}{\pi^{1/2}\Gamma(n)}, \quad (7)$$

for the Laplace distribution, with $\Gamma(\cdot)$ denoting the Gamma function or generalized factorial. For the Student $t(3)$ distributed innovations

$$E(|r_t^n|) = \frac{2\sqrt{3}}{\pi} \left(n - (n-1) \sum_{k=0}^{n-2} \frac{(n-2)!}{(n-2-k)!(k+1)(k+2)n^k} \right). \quad (8)$$

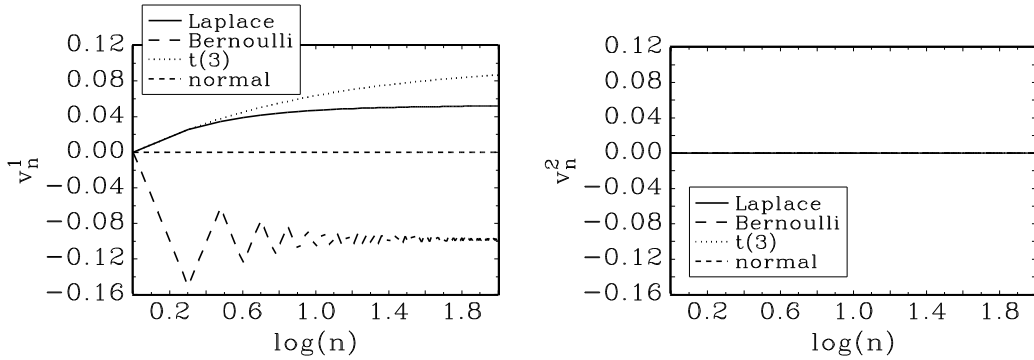


Figure 1: Analytical first absolute moment ratio curves (left-hand panel) and variance ratio curves (right-hand panel) for normal, Laplace, Student- $t(3)$, and shifted Bernoulli distributed ε_t .

For the shifted Bernoulli distribution

$$E(|r_t^n|) = \frac{2^{-n}n!}{\lfloor \frac{n}{2} \rfloor! \lfloor \frac{n-1}{2} \rfloor!}, \quad (9)$$

where $\lfloor x \rfloor$ denotes the integer part of x , also known as the entier function. Appendix B also proves for each of these distributions that $E(|r_t^n|) \stackrel{a}{\sim} n^{1/2}$ for $n \rightarrow \infty$, illustrating the validity of Theorem 1 for these example distributions. Plots of the volatility ratio curves v_n^1 and v_n^2 versus $\log(n)$ for the above distributions are provided in Figure 1. Note that we use the base-10 logarithm, so that $\log(100) = 2$ refers to a 100 period convolution of single returns.

It is clear in Figure 1 that the first absolute moment ratio curves for the fat-tailed distributions lie above that of the normal distribution. In contrast, the curve for the shifted Bernoulli lies below that of the normal. The applicability of Theorem 2 now follows from the fact that $E(|\varepsilon_t|)/(E(\varepsilon_t^2))^{1/2}$ equals $2^{-1/2}$, $2/\pi$, and 1 for the Laplace, the Student $t(3)$, and the shifted Bernoulli, respectively. The moment ratio curves based on absolute returns ($\zeta = 1$) can therefore be used to distinguish between fat-tailed and thin-tailed distributions. Note again that variance ratio curves ($\zeta = 2$) contain no information whatsoever in this respect. Furthermore, as follows from Theorem 1, all curves in the left-hand panel of Figure 1 level off for sufficiently large values of n , and eventually become horizontal. For extremely fat-tailed distributions like the Student $t(3)$, however, the return horizon n for which the curve becomes horizontal may be excessively large given the sample size typically available in empirical work.

2.3 Volatility clustering

The assumption of i.i.d. one-period returns does not fit typical financial data. Such data often exhibit forms of volatility clustering. In this subsection we concentrate on the effect of autoregressive conditional heteroskedasticity (ARCH) on moment ratio curves. It is well known that even if the innovations to the ARCH process are (conditionally) normal, the unconditional distribution (stationary distribution) is heavy-tailed, see Engle (1982), de Haan et al. (1989), and Nelson (1990). The following theorem summarizes what pattern we can expect for the volatility ratio curves in case of ARCH.

Theorem 3 (Volatility clusters) *Let the return innovations follow a finite variance normal ARCH(p) process*

$$\begin{aligned}\varepsilon_t &= h_t^{1/2} x_t, \quad x_t \text{ i.i.d. } N(0, 1), \\ h_t &= \omega + \sum_{i=1}^p \lambda_i \varepsilon_{t-i}^2, \quad \omega > 0, \lambda_i > 0, \sum_i \lambda_i < 1.\end{aligned}$$

Then $v_n^2 \equiv 0$, while $v_n^1 > 0$ for sufficiently large n .

The proof can be found in Appendix A. Note that covariance stationary GARCH(1,1) processes can also be handled through the above method of proof. If the innovations x_t in the ARCH process are not $N(0, 1)$, then the LHS of (A.3) in the proof of Theorem 3 becomes a composite product of the ratio $E(\sqrt{h_t})/\sqrt{E(h_t)}$ and $E(|x_t^1|)/\sqrt{E((x_t^1)^2)}$. The latter also appeared in Theorem 2. Hence, if the innovations x_t are also heavy-tailed in the sense of Theorem 2, then the conclusion of Theorem 3 is reinforced. In contrast, if the innovations are light-tailed, the inequality (A.3) with $\zeta = 1$ may be reversed.

Note that a heavy-tailed distributed x_t and a nonzero λ both have the effect of raising v_n^1 above zero. So if $v_n^1 > 0$ is observed, it is not possible to tell whether this is caused by fat tails or volatility clustering. Fortunately, for small n , volatility clustering has a rather distinct effect on v_n^1 in comparison to the heavy tail effect. This is the upshot of the next theorem.

Theorem 4 *Let ε_t follow a covariance stationary ARCH(1) process as in Theorem 3, but where the i.i.d. innovations x_t follow any symmetric distribution around 0 with finite variance $\sigma^2 < \infty$. Let $v_{n,\lambda}^1$ denote the moment ratio curve based on $\zeta = 1$ with ARCH(1) parameter $\lambda_1 = \lambda$. If $\lambda > 0$, then eventually $v_{n,\lambda}^1 > v_{n,0}^1$ as $n \rightarrow \infty$. But for $n = 2$, the converse result is that*

$$\left. \frac{\partial v_{2,\lambda}^1}{\partial \lambda} \right|_{\lambda=0} < 0.$$

The proof to this claim is given in Appendix A. The result is that the effect of volatility clusters on the v_n^1 curve is markedly different from the effect of fat-tailed i.i.d. innovations. In particular, the volatility clustering causes a downward (upward) shift in the moment ratio curve based on absolute returns for small (large) values of n compared to the i.i.d. case. So, for a certain range of return horizons n , the slope of the moment ratio curve under volatility clustering will initially be below that of the corresponding i.i.d. case. Afterwards, the slope will be larger. Below, we will exploit these properties to extract information concerning the heavy tail feature and the volatility clustering effect from the absolute moment ratios.

Remark 2 There are alternative modelling strategies to capture the volatility clustering effect like stochastic volatility. For a stochastic volatility process one can show an analogous result to Theorem 3. Moreover, for short horizons the absolute moment ratio dips below the i.i.d. based curve. For the sake of brevity, we omit a detailed treatment.

2.4 Linear dependence

Theorems 2 through 4 illustrate settings in which the variance ratio plots ($\zeta = 2$) are informative only when used in conjunction with volatility ratio curves based on $\zeta = 1$. We now consider the case where the volatility ratio curves for both $\zeta = 1$ and $\zeta = 2$ are informative. This case is also treated in the standard literature on variance ratio tests. The following theorem summarizes the result.

Theorem 5 *Let ε_t follow a covariance stationary invertible ARMA process with absolutely summable autocovariances $\gamma_j = \text{cov}(r_t^1, r_{t-j}^1)$, $\sum_{j=0}^{\infty} |\gamma_j| < \infty$. Then*

$$v_n^\zeta \geq 0$$

is equivalent to

$$E(|\xi|^\zeta) \geq \frac{E(|\varepsilon_t|^\zeta)}{E((\varepsilon_t)^2)^{\zeta/2}} \left(\frac{\gamma_0}{\sum_{j=-\infty}^{\infty} \gamma_j} \right)^{\zeta/2}, \quad (10)$$

with ξ a standard normal random variate.

The proof is again in Appendix A. Comparing Theorem 5 with the previous theorems, we note that there is an additional factor on the RHS in (10). So even if the innovations to the ARMA process are normally distributed

such that $E(|\varepsilon_t|^\zeta)/E(\varepsilon_t^2)^{\zeta/2} = E(\xi^\zeta)$, the factor $(\gamma_0/\sum_{j=-\infty}^{\infty}\gamma_j)^{\zeta/2}$ on the RHS of (10) remains. For the remainder of the discussion, we focus on $\zeta = 2$. Plots for $\zeta = 1$ reveal a similar pattern. But the plot for $\zeta = 1$ is more ambiguous, because deviations are also caused by other factors than linear dependence, see Sections 2.2 and 2.3. For $\zeta = 2$, the additional factor in (10) equals the ratio of the short term variance of the one-period return process to the long-run variance, see, e.g., Ibragimov and Linnik (1971, Theorem 18.2.1) and Phillips (1987). Define

$$\bar{\sigma}^2 = \sum_{j=-\infty}^{\infty} \gamma_j = \lim_{n \rightarrow \infty} \frac{(\sum_{i=1}^n \varepsilon_i)^2}{n},$$

and $\sigma^2 = \gamma_0$. Then (3) reduces to $\log(\bar{\sigma}^2/\sigma^2) + \log(n)$ for large values of n . Note that this curve has the same slope as for i.i.d. returns, namely 1 (see also Theorem 1), but that the level of the curve has shifted with respect to the i.i.d. case. For a positive long-run correlation of the ε_t ($\bar{\sigma}^2 > \sigma^2$) the variance ratio curve lies above the i.i.d. one, while for negative long-run correlations ($\bar{\sigma}^2 < \sigma^2$) the opposite holds. This is easily illustrated using AR(1) one-period returns with autoregressive parameter φ . In that case, (10) becomes $1 \geq [(1 - \varphi)/(1 + \varphi)]$, such that $v_n^2 \geq 0$ for $\varphi \geq 0$. Plots of volatility ratio curves for correlated returns are found in Groenendijk et al. (1997).

Note that the above line of reasoning is only valid conditional on $\bar{\sigma}^2$ being strictly positive. If there is a moving average unit root in the return process, then $\bar{\sigma}$ is zero, such that the moment ratio curve v_n^2 defined in (5) decreases for large values of n . To illustrate such behavior, consider an ARMA(1,1) process for log asset prices p_t ,

$$p_t = \varphi p_{t-1} + \varepsilon_t - \theta \varepsilon_{t-1}, \quad (11)$$

with ε_t i.i.d. standard normal random variables. Let $|\varphi| < 1$, such that asset returns have a moving average unit root, i.e., $r_t^1 = \varphi r_{t-1}^1 + \tilde{\theta}(L)\varepsilon_t$, with $\tilde{\theta}(L) = (1 - L)(1 - \theta L)$, L the lag operator $L\varepsilon_t = \varepsilon_{t-1}$, and $\tilde{\theta}(1) = 0$. It is proved in Appendix B.4 that

$$E((r_t^n)^2) = \frac{2(1 - \varphi^n)(1 - 2\theta\varphi + \theta^2)}{1 - \varphi^2} + 2\theta\varphi^{n-1}, \quad (12)$$

which is bounded uniformly in n . Consequently, the long-run variance $\bar{\sigma}^2 = \lim_{n \rightarrow \infty} E((r_t^n)^2)/n = 0$. Moreover, the variance ratio curve ($\zeta = 2$) clearly decreases for n sufficiently large, as is shown in the right-hand panel of Figure 2. Because for normal innovations the expectation of the absolute n -period return is proportional to the square root of (11), with the constant

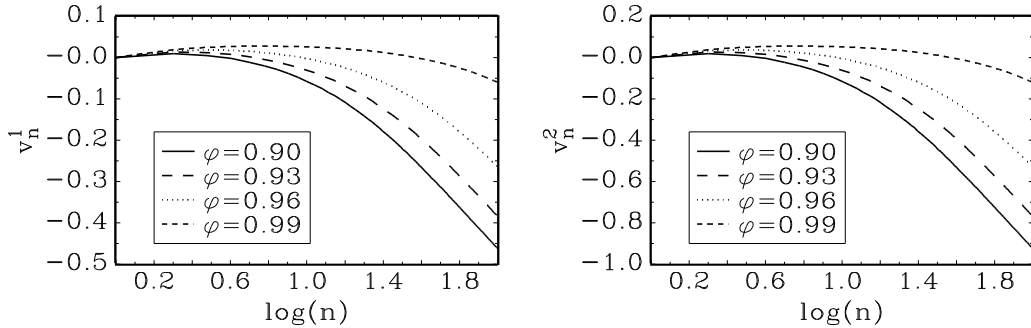


Figure 2: Analytical first absolute moment ratio curves (left-hand panel) and variance ratio curves (right-hand panel) for the autoregressive log asset price process in (11), where $\theta = -0.1$ and φ as indicated.

of proportionality independent of n , similar features hold for the volatility ratio curves based on $\zeta = 1$, as shown in the left-hand panel of Figure 2. So linear dependence of returns becomes apparent through either a level shift in the volatility ratio curve or a decline of the curve in $\log(n)$, both in the $\zeta = 1$ and $\zeta = 2$ plots.

2.5 Conclusion and interpretation of related results

Subsections 2.2 through 2.4 illustrate that standard variance ratio tests can only effectively distinguish between correlated and uncorrelated asset returns. In contrast, when these tests are used in conjunction with moment ratio curves based on absolute returns, our results show that useful information may be obtained both on linear and non-linear dependence in asset returns and on thin-tailedness or fat-tailedness. By recognizing the joint pattern of moment ratio curves for $\zeta = 1$ and $\zeta = 2$, the graphical representation of moment ratio curves laid out in this section can be used to obtain an assessment of the salient features of asset returns. This, together with the formal statistical tests explained in Section 3, turns the approach into a hybrid testing procedure for disentangling non-normality, first moment dependence, and second moment dependence in asset returns.

To conclude this section we comment on related work in the literature. Moment ratio curves based on absolute returns are implicit in Müller et al. (1990) and Guillaume et al. (1997) as a tool for exploratory data analysis. Our formal results derived in this section shed new light on their results. In Müller et al. (1990) and Guillaume et al. (1997) large tic-by-tic data sets on forex quotes are used to plot averages of $|r_t^n|$ against $\ln(n)$. Hence, the slope in such plots implicitly provides a measure of V_n^1 , since the slope measures

$\sqrt{n}V_n^1$ (if the variance is bounded). These studies report slope estimates which hover around 0.58, and Müller et al. note that these estimates are well above the 0.50 which can be expected if the returns are i.i.d. Gaussian distributed. This deviation from normality in the slope estimates is referred to as the scaling law. In principle two sorts of causes may explain the scaling law. One explanation would be that the i.i.d. innovations are so heavy tailed that $\alpha < 2$. On basis of Theorem 1, the slope estimate of 0.58 would then correspond to an $\alpha = 1.72$. Another explanation would be that the returns are non-i.i.d. or are non-normally distributed but with $\alpha = 2$. In the latter case, for example, the LHS panel of Figure 1 shows that the slope eventually approaches 0.50, but deviates from 0.50 at the higher frequencies. Regression analysis such as are used in the referenced studies can then easily produce slope estimates above 0.50, especially so if ultra-high frequency data are used. In the application section we provide evidence for the latter explanation behind the scaling law.

3 Joint inference on volatility ratios

As was mentioned earlier, the graphical representation of the moment curves as put forward in Section 2 can be used to detect various features of asset returns, e.g., fat-tailedness, linear dependence, and non-linear dependence, by recognizing the patterns of these curves. In this section we construct a formal statistical testing procedure to complement the information contained in the graphical plots. Our approach is hybrid in character, mixing formal statistical tests with expert opinions based on exploratory data analysis using moment ratio curves.

Standard variance ratio tests are usually computed for different return horizons. In fact, one of the main puzzles stemming from the application of these tests is the possible presence of positive autocorrelation at short horizons, and negative correlation at long horizons, see, e.g., Fama and French (1988) and Poterba and Summers (1988). Chow and Denning (1993) and Fong et al. (1997) recently argued that variance ratio tests for different return horizons based on a single data set require modifications of the inference procedure. In particular, standard confidence intervals for the tests have to be widened if more than one test is computed using the same data set. This is due to the fact that volatility ratios for different return horizons are generally imperfectly correlated. We account for this phenomenon in developing a formal inference procedure for our generalized moment ratio test. We advocate a graphical presentation of the test. In this way we establish a close link between the formal test procedure of the present section and the shapes

of the moment ratio curves established in the previous section. This proves especially helpful if standard variance ratio tests are used in conjunction with tests based on alternative measures of volatility.

Using the notation of the previous section, we consider a set of N moment ratios, indexed as

$$\hat{V}_n^\zeta = \frac{T \sum_{t=n}^T |r_t^n|^\zeta}{n^{\zeta/\alpha} (T+1-n) \sum_{t=1}^T |r_t^1|^\zeta}, \quad (13)$$

for $n = 1, \dots, N$. Note that \hat{V}_n^ζ is a natural estimator of V_n^ζ in (6). The estimate is based on overlapping n -period returns using a sample of T one-period returns. Let $\hat{v}_n^\zeta = \log(\hat{V}_n^\zeta)$, where \log is the base-10 logarithm. The empirical counterpart of the curves presented in Section 2 is a plot of \hat{v}_n^ζ versus $\log(n)$ for $n = 1, \dots, N$. According to Theorem 1 this curve should become horizontal for large values of n . Moreover, if the r_t^1 are i.i.d. α -stable distributed, the curve should be approximately zero over its entire domain, see Equation (4). In order to derive a formal testing procedure, we need some type of confidence bands for the \hat{v}_n^ζ -curve. The usual approach found in the literature is to construct pointwise confidence intervals for each value of n . Such confidence bands suffer from the fact that the different points on the \hat{v}_n^ζ -curve are computed using the same data. As moment ratios for different return horizons are imperfectly correlated, using pointwise confidence bands results in a testing procedure that is oversized. Chow and Denning (1993) solve this problem by a Bonferroni argument using the Studentized Maximum Modulus (SMM) distribution. We argue that their approach is too conservative in general, as the SMM distribution does not account for the high correlation between different v_n^ζ 's that arises (especially) for large n . Moreover, their simultaneous inference procedure does not allow for an easily tractable analytical analogue in case different volatility measures are used than the variance, i.e., if $\zeta < 2$. Therefore, we base our simultaneous or *uniform* (in the return horizon n) confidence bands on bootstrap estimates. This approach has two main advantages. First, it can be implemented for general values of α and ζ . Second, it accounts for the simultaneity problem without resorting to procedures that are generally too conservative given the structure of the testing problem. A disadvantage of the bootstrap is the increase in computation time.

We propose the use of different bootstrap procedures in the $\zeta = 2$ and the $\zeta = 1$ plots. This follows from the different information that can be obtained from these plots. Whereas the $\zeta = 2$ plot is mainly suited for detecting deviations from the martingale hypothesis, the $\zeta = 1$ plot is useful for detecting tail behavior and volatility clustering. Subsection 3.1 treats the

formal inference procedure for $\zeta = 2$, while Subsection 3.2 discusses the use of the bootstrap for $\zeta = 1$ based moment ratio curves.

Before we explain the details of our bootstrap procedures, we comment on the choice of the stability parameter α in (13). A specific value of α is needed in order to make the inference procedure operational. The choice of α affects the slope of the moment ratio curve for large n . For a correct choice of α , Theorem 1 shows that the curve ultimately becomes horizontal. Unless explicitly stated otherwise, we assume for the remainder of this paper that $\alpha = 2$. This is motivated by the fact that there seems to be some consensus in the literature that at least second moments exist for most financial time series, see Pagan (1996). Note, however, that even if α turns out to be smaller than 2, the first absolute moment ratio curve and our bootstrap methodology still provide useful information about the properties of the observed series. Care must be taken, however, in assessing the validity of the formal inference procedure in such cases.

3.1 The block-bootstrap and $\zeta = 2$

The plot for $\zeta = 2$ is useful for detecting deviations from the martingale assumption. Therefore, a formal statistical test should allow for the possibility that the return series has non-linear dependence, e.g., volatility clustering. Apart from this, we also have to cope with two additional complexities in deriving an appropriate inference procedure. First, we have to account for the fact that overlapping data are used to compute the different points on the moment ratio curve. Second, even if we were to use non-overlapping data, we have to account for the fact that the different points on the moment ratio curve are not independent, because they are based on the same data set. A simultaneous and analytical treatment of all the above topics appears extremely difficult and can, to our knowledge, not be found in the literature. Therefore we adopt a simulation based inference procedure using the bootstrap.

In order to account for the possible dependence in the returns, we use a block-bootstrap procedure. The approach is as follows. Given a sample of one-period returns $\{r_t^1\}_{t=1}^T$, we draw a bootstrap sample $\{r_t^{1,b}\}_{t=1}^T$ by randomly drawing blocks (with replacement) of length m from the original one-period returns r_t^1 . A block consists of m consecutive returns: $r_t^1, \dots, r_{t+m-1}^1$. The blocks can be overlapping. If the sample size T is not an integer multiple of the block size m , only the first part of the final block drawn is used to construct the bootstrap series. As a result, the bootstrap sample also contains T one-period observations. For a specific bootstrap sample, we compute the bootstrapped moment ratio curve $\hat{v}_n^{\zeta,b}$. This can be done a large, say B ,

number of times.

Given the sample of bootstrapped volatility ratio curves, we compute

$$\bar{v}_n^\zeta = B^{-1} \sum_{b=1}^B \hat{v}_n^{\zeta,b}, \quad (14)$$

$$\bar{\sigma}_n^\zeta = B^{-1} \sum_{b=1}^B (\hat{v}_n^{\zeta,b} - \bar{v}_n^\zeta)^2, \quad (15)$$

and

$$\widehat{sv}_n^{\zeta,b} = (\hat{v}_n^{\zeta,b} - \bar{v}_n^\zeta) / \bar{\sigma}_n^\zeta. \quad (16)$$

We call $\widehat{sv}_n^{\zeta,b}$ the standardized moment ratio curve, and \bar{v}_n^ζ is called the average bootstrap curve. Based on the standard moment ratio curves, we compute the uniform bounds low^ζ and up^ζ such that

$$low^\zeta = \sup_l \left\{ l \mid \#\{b \mid \exists n : \widehat{sv}_n^{\zeta,b} < l\} \leq \alpha^* B/2 \right\} \quad (17)$$

and

$$up^\zeta = \inf_u \left\{ u \mid \#\{b \mid \exists n : \widehat{sv}_n^{\zeta,b} > u\} \leq \alpha^* B/2 \right\}, \quad (18)$$

where α^* is the desired significance level of the (joint) moment ratio test, and $\#A$ denotes the number of elements in the set A . Unless the \hat{v}_n^ζ -curves of the observed process are highly non-monotonic, the above approach will approximately provide the correct coverage level asymptotically. Otherwise, our approach will be slightly conservative. Given the typical pattern for volatility plots in Sections 2 and 4 for processes that can be thought relevant for financial data, however, we do not think that this problem will be important for practical purposes. We investigate this claim by means of simulation in the next section. The uniform upper and lower confidence bands of the moment ratio curve \hat{v}_n^ζ are computed as $\bar{v}_n^\zeta + low^\zeta \cdot \bar{\sigma}_n^\zeta$ and $\bar{v}_n^\zeta + up^\zeta \cdot \bar{\sigma}_n^\zeta$, respectively. We plot these bands and the average bootstrap curve \bar{v}_n^ζ along with the empirical curve \hat{v}_n^ζ in one figure.

Using the above procedure, we deal with the overlapping data problem as well as with the simultaneity problem, while allowing for phenomena as volatility clustering by using the block-bootstrap. The length of the blocks used is, of course, both a theoretical and an empirical matter. In the computations for the present paper we use blocks of length 10. We also experimented with blocks of length 5 and 20 without substantial changes in the

results. Asymptotically, of course, we require the block length to diverge to infinity with the sample size at an appropriate rate, see Hall et al. (1995) and Shao and Tu (1995). We leave this for further research. Ideally, we would like an automated optimal block-length selection in finite samples, but this would unduely increase the required computation time.

We expect the following from our formal inference procedure. If the martingale assumption is satisfied, the entire $\log(n)$ -axis should be contained in the confidence band, irrespective of whether the returns are thin-tailed or fat-tailed or whether or not they exhibit volatility clustering. If the returns are linearly dependent, we expect that (part of) the $\log(n)$ -axis falls outside the confidence band. For independent returns, moreover, we expect that the empirical curve lies inside the confidence band. This is not so evident for the case of non-linearly dependent returns. Though the dependence structure is captured correctly asymptotically by the use of the block-bootstrap, in finite samples the correlation structure may be corrupted. This is especially relevant near the end points of the blocks. If (non-linear) dependence is strong, the bias caused by the finite block length in the block-bootstrap procedure may be significant, see, e.g., Section 4.

3.2 The i.i.d.-bootstrap and $\zeta = 1$

In our methodology, we augment the standard variance ratios with alternative moment ratios based on absolute returns. As mentioned in Section 2, plots of moment ratio curves for $\zeta = 1$ complement the information contained in curves for $\zeta = 2$. The plots based on absolute returns ($\zeta = 1$) are especially useful for detecting deviations from normality and non-linear independence. So whereas the implicit null hypothesis for the $\zeta = 2$ plots is the martingale model, for the $\zeta = 1$ plots it is the i.i.d. normal model. This difference in implicit null hypotheses requires a different bootstrap methodology. Whereas we used the block-bootstrap for the $\zeta = 2$ curve in order to allow for possible non-linear dependence in the returns, we can use the i.i.d. bootstrap in case $\zeta = 1$. The formal methodology is identical to the one described in the previous subsection for $\zeta = 2$, only with the block size m set equal to 1.

If the one-period returns are normal and i.i.d., we expect both the empirical moment ratio curve and the $\log(n)$ -axis to be covered completely by the bootstrapped confidence band. In contrast, if the returns are sufficiently non-normal and i.i.d., we expect the $\log(n)$ -axis to fall outside the confidence band for certain values of n . The empirical curve in that case, however, should still be contained in the confidence band, see Section 2. For a sufficiently high degree of non-linear dependence, e.g., volatility clustering, we expect that parts of both the $\log(n)$ -axis and the empirical curve fall

outside the confidence band. For volatility clustering, and since the $\zeta = 1$ bootstrap uses an i.i.d. resampling scheme, the clustering induces positive bootstrapped volatility ratio curves on average (due to the fat-tailedness of the unconditional distribution). As a result, the $\log(n)$ -axis is likely to fall outside the confidence band. Moreover, as was demonstrated in Section 2.3, ARCH effects result in a downward sloping moment ratio curve for small n . This effect is not captured by the i.i.d. resampling scheme, such that we can expect the empirical curve to fall outside (below) the confidence band for certain small values of the return horizon n . Note that in all cases described above, we also expect the $\zeta = 2$ curve not to signal any deviations from the martingale model.

Finally, if returns are linearly dependent, we expect that the confidence band fails to cover the empirical curve for $\zeta = 1$. Two other things should be noted in this case for the $\zeta = 1$ plot. First, though the resampling scheme is i.i.d., there may be a bias in the average bootstrap curve for $\zeta = 1$ if the linear dependence is sufficiently strong. This is intuitively clear, as in that case the one-period returns may still be correlated, even if the returns are relatively far apart in time. Second, even in case the returns are linearly dependent, the average bootstrapped volatility ratio curve for $\zeta = 1$ still contains useful information concerning the tail behavior of the returns. Abstracting for the moment from the bias discussed earlier, the i.i.d. resampling scheme gives a signal concerning the unconditional tail behavior of the returns. If one only allows for linear dependence, this directly reveals information on the tail behavior of the innovations to the return process. Alternatively, if one also allows for non-linear dependence, the average bootstrapped curve may signal non-normal unconditional tail behavior. Given the typical sample size and correlation structure found in financial return series, we think that the effect of the bias mentioned in the first remark above will be quite limited. For the same reason, we conjecture that the information content of the average bootstrap curve for $\zeta = 1$ may still be significant in many situations of practical interest.

4 Monte-Carlo illustrations

In this section we further illustrate the properties of our new hybrid testing procedure using simulated time series. We consider four sets of simulations. First, we consider normal i.i.d. one-period returns. This case serves as the benchmark. Second, we investigate the effect of fat-tailedness by generating i.i.d. one-period returns from the Student $t(3)$ distribution. Our last two sets of simulations concern the behavior of the tests under linear and second

order dependence in the one-period returns, respectively.

In all set-ups used below, we consider two experiments. In the first experiment, we consider a single representative realization of a time series of length $T = 1,000$ and moment ratios up to horizon $N = 100$. This experiment aims at giving insight into what patterns of moment ratio curves to expect in situations of practical interest. For $\zeta = 1$, the number of bootstrap simulations is $B = 1,000$, while for $\zeta = 2$, we perform $B = 1,000$ block-bootstrap simulations using blocks of length 10. The nominal significance level of the formal test is $\alpha^* = 0.05$. As mentioned in Section 3, we assume that the variance of the returns exists, i.e., $\alpha = 2$. The results of the first experiment are complemented by a second experiment, which presents a limited study on the power of our hybrid testing procedure. In this second experiment, we perform 100 Monte-Carlo replications of the first experiment. For each Monte-Carlo simulation, we record at what return horizon the empirical moment ratio curve or the $\log(n)$ -axis falls outside the bootstrapped confidence band. We report the average rejection frequencies over the Monte-Carlo samples. The number of Monte-Carlo simulations was limited to 100. As each Monte-Carlo simulation involves 1,000 bootstraps for $\zeta = 1$ and yet another 1,000 for $\zeta = 2$, the total computation time of these Monte-Carlo simulations rises rapidly.

4.1 Normal i.i.d.

The result for normal i.i.d. returns is presented in Figure 3. In the upper panels, we see that both the empirical volatility ratio curve (\hat{v}_n^ζ) and the $\log(n)$ -axis fall well within the uniform confidence band, both for $\zeta = 1$ and $\zeta = 2$, such that we have no indication of fat-tailedness or dependence in the one-period returns. Although the empirical volatility ratio curve seems to display some non-monotonic behavior, the effect is not significant given the confidence bands. The lower panels of the figure demonstrate that the formal statistical test is somewhat undersized if we consider pointwise rejection frequencies. For uniform rejection frequencies, however, the test appears to be somewhat oversized as $0.11 > 0.05$. The empirical curve thus appears to lie outside the confidence band too often compared to the nominal size of the test. Due to the limited number of simulations for the lower panels, however, these conclusions are only indicative.

4.2 Student $t(3)$ i.i.d.

We now turn to the case of Student $t(3)$ i.i.d. one-period returns. The results are presented in Figure 4. First, consider the $\zeta = 2$ plot of the upper panels in Figure 4, i.e., the variance ratio curve. Both the empirical curve and

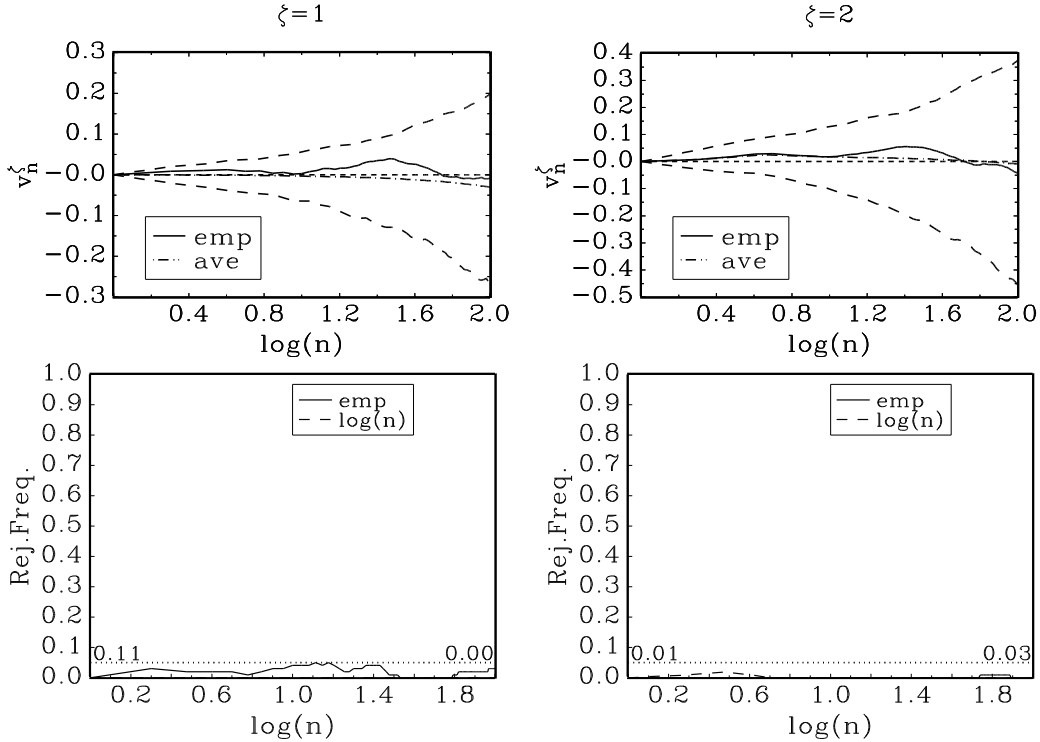


Figure 3: The upper panels display simulated moment ratio curves for a single batch of normally distributed ε_t , with (block-)bootstrapped uniform confidence bands. The lower panels present the pointwise frequencies by which the empirical volatility ratio curve or the $\log(n)$ -axis fall outside the uniform confidence band for $\zeta = 1$ and $\zeta = 2$, respectively. The left-hand and right-hand numbers inside the (lower) plots give the uniform rejection frequencies over the Monte-Carlo replications of the empirical and the $\log(n)$ -axis falling inside the confidence band, respectively.

the $\log(n)$ -axis lie well within the confidence band. From this we conclude that there is no significant indication of linear dependence in the returns, hence the martingale hypothesis cannot be rejected. Note, however, that the confidence bands for $\zeta = 2$ have to be interpreted with care, as fourth order moments of the Student $t(3)$ distribution do not exist. To obtain information about fat-tailedness and non-i.i.d.-ness, we turn to the plot based on $\zeta = 1$. While the empirical curve falls entirely within the band, part of the $\log(n)$ -axis lies below the confidence band. As explained in Section 2.2, this signals deviations from normality. Since the confidence band in the $\zeta = 2$ plot contains the $\log(n)$ -axis, i.i.d.-ness is maintained. Also note that the average bootstrap curve lies entirely above the $\log(n)$ -axis, again signalling fat-tailedness. However, given that the empirical curve stays within the band,

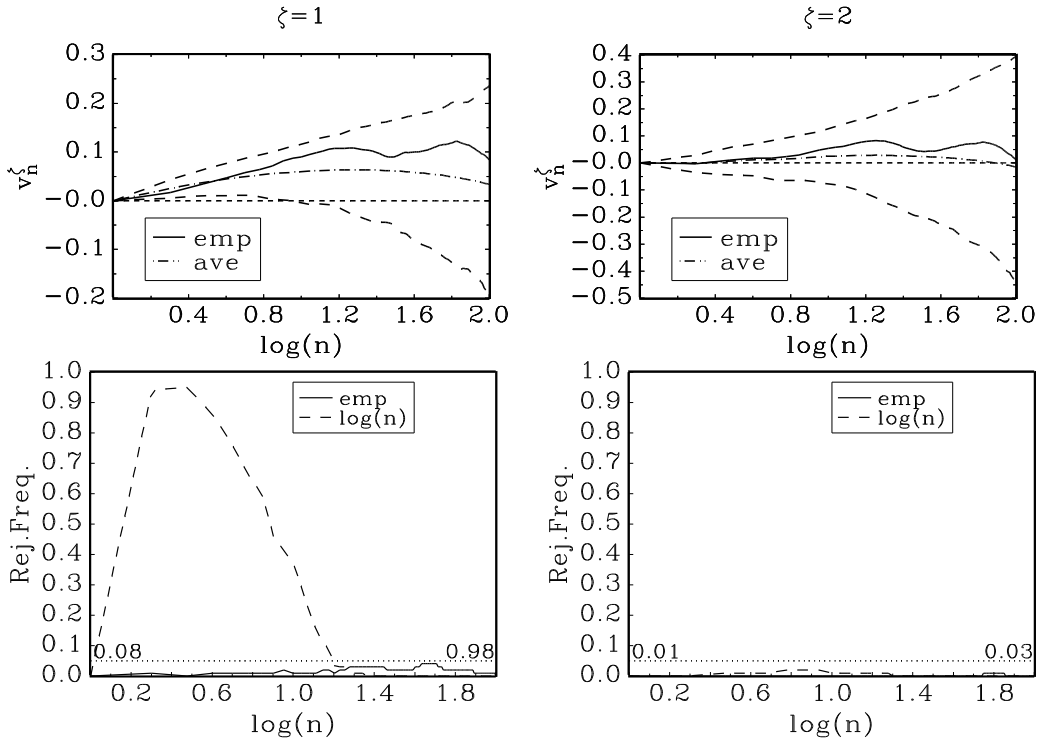


Figure 4: Results for simulated moment ratio curves for Student $t(3)$ distributed ε_t ; see the note to Figure 2 for a description of the contents.

there is no volatility clustering. Of course this is exactly what we would expect given the nature of the generated return series.

The lower panels in Figure 4 again demonstrate the performance of our test procedure for Student $t(3)$ innovations over repeated experiments. As expected, the variance ratio curves ($\zeta = 2$) have no ability to distinguish between thin-tailed and fat-tailed martingales. The empirical uniform rejection frequencies (0.01 and 0.03) are somewhat below the nominal size of the test. In contrast, the empirical rejection frequencies for $\zeta = 1$ are much more interesting. The uniform rejection frequency for the empirical curve falling inside the confidence band (0.08) is close to the nominal size of 0.05. This illustrates that no significant departures from the i.i.d.-assumption are found. The probability of the $\log(n)$ -axis falling outside the confidence band, however, is extremely high (0.98), illustrating that our procedure has power in discriminating thin-tailed from fat-tailed martingales. The pointwise rejection frequencies illustrate that the confidence band for the $\zeta = 1$ moment ratio curves fails to cover the $\log(n)$ -axis for return horizons between 1 and 15. This again corroborates the patterns displayed in the upper panels of

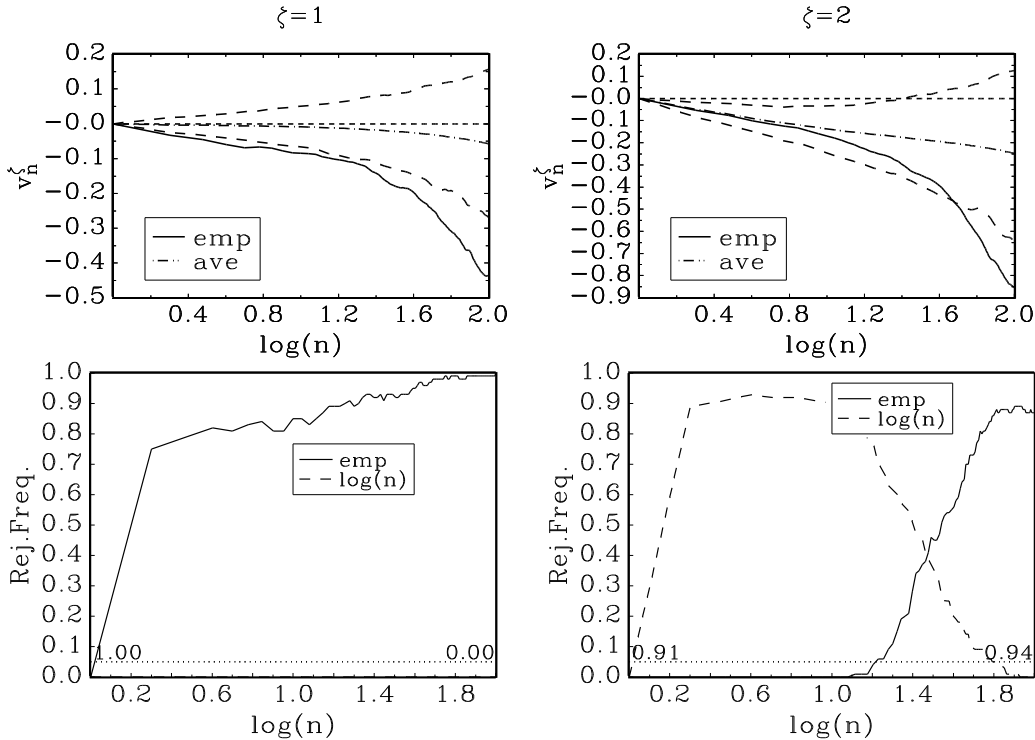


Figure 5: Results for simulated volatility ratio curves for the ARMA log price process in (19); see the note to Figure 3 for a description of the contents.

Figure 4.

4.3 ARMA(1,1) log prices

We now abstract from the i.i.d. assumption and consider dependent one-period returns. Consider an ARMA(1,1) for the log price level,

$$p_t = 0.95p_{t-1} + \varepsilon_t - 0.1\varepsilon_{t-1}, \quad (19)$$

with ε_t i.i.d. standard normal. The result is presented in Figure 5.

We see that the empirical volatility ratio curve falls well outside the confidence region, both for $\zeta = 1$ and $\zeta = 2$. This clearly signals linear dependence in the returns, as explained in Section 3.1. Also note that for $\zeta = 2$, the $\log(n)$ -axis partly falls outside the confidence band, which confirms the presence of linear dependence. For $\zeta = 1$, in contrast, the $\log(n)$ -axis lies well inside the band, which is what we would expect given the i.i.d. bootstrap method used in that case. Some additional information may be obtained from the average bootstrap curve in the $\zeta = 1$ plot. Since this curve lies

close to the $\log(n)$ -axis, we conclude that we detect significant departures from the assumption of i.i.d. returns, but no deviations from the assumption of normality.

The lower panels in Figure 5 support these findings. Uniform rejection frequencies for the $\zeta = 2$ plot are both high (0.91 and 0.94). The fact that the $\log(n)$ -axis falls outside the confidence band with high probability signals that uncorrelatedness is strongly rejected. For long return horizons n , we also note that the empirical curve often falls outside the confidence band. This is a consequence of the block-bootstrap methodology used. As blocks of length 10 are used in the simulations, we cannot expect the correlation structure of the original series to be captured beyond return horizons of 10 periods. The correlation between distant returns may be far larger than the correlation implied by the block-bootstrap. This is the case in our simulation set-up, as demonstrated by the high pointwise rejection frequencies for large n . The lower-left panel in Figure 5 also reveals some interesting patterns. Again, the uniform rejection frequency for the empirical curve falling inside the confidence band is extremely high (1.00), especially for large return horizons. The rejection frequency for the $\log(n)$ -axis falling inside the band, in contrast, are extremely low (0.00). So from the $\zeta = 1$ plot we conclude deviations from i.i.d.-ness, but no deviations from normality. Combining this with the $\zeta = 2$ plot, we additionally conclude that the departures from i.i.d.-ness are caused by deviations from the martingale assumption and not by ARCH effects. The latter conclusion follows from the observation that ARCH effects would imply large rejection frequencies for the $\log(n)$ -axis falling outside the confidence band for $\zeta = 1$, something we demonstrate next.

4.4 ARCH

To conclude this section, we consider a situation in which the martingale assumption is valid, but the independence assumption is violated. This case is of special interest in financial applications, where researchers often find volatility clustering for asset returns, see, e.g., Pagan (1996) for references. As a simple illustration of the effect of volatility clustering on our hybrid testing procedure, we consider an ARCH process of order one: $r_t^1 = h_t^{1/2} \varepsilon_t$, with

$$h_t = 0.01 + 0.95\varepsilon_{t-1}^2, \quad (20)$$

and ε_t a set of i.i.d. standard normal random variables. The results are presented in Figure 6.

In the $\zeta = 2$ plot we see that both the empirical curve and the $\log(n)$ -axis lie within the confidence band. Though the empirical curve is non-monotonic,

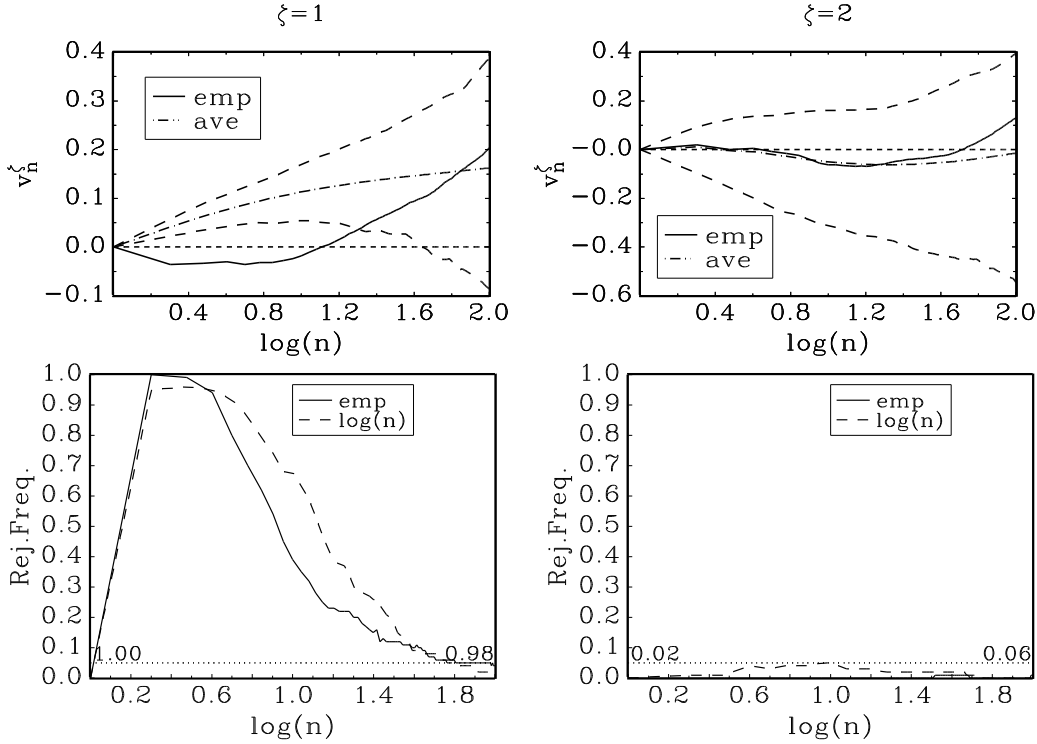


Figure 6: Results for simulated moment ratio curves for the ARCH process in (20); see the note to Figure 3 for a description of the contents.

the effect does not appear to be significant. Thus, the martingale hypothesis cannot be rejected, i.e., there is no dependence in the first moment. Again, the $\zeta = 1$ plot reveals additional information about the data. A large part of the $\log(n)$ -axis falls outside the confidence interval. This points to volatility clustering and/or non-normality. Since the empirical curve lies below the lower confidence band for small values of n , we conclude that the returns exhibit ARCH effects. The fact that the empirical curve lies below the $\log(n)$ -axis for small n , and above the $\log(n)$ -axis for larger n corroborates our theoretical results of Theorem 4. Furthermore, we know from the literature that the unconditional distribution of a conditionally normal ARCH process is leptokurtic, see, e.g., Nelson (1990). This is clearly revealed by the average bootstrap curve shown in the $\zeta = 1$ plot.

The results for the single experiment presented in the upper panels of Figure 6 are strongly supported by the findings over repeated experiments, as reported in the lower panels. The panel for $\zeta = 2$ demonstrates that the nominal size of the test (0.05) is close to its empirical (uniform) size for ARCH processes (0.02 and 0.06 for the empirical curve and the $\log(n)$ -axis,

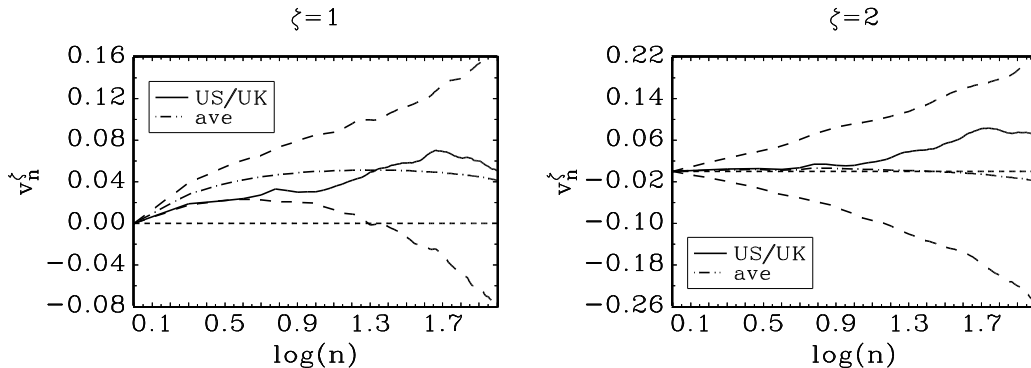


Figure 7: *Moment ratio curves for the US/UK exchange rate from January 3, 1986 to December 31, 1997, with (block-)bootstrapped uniform confidence intervals.*

respectively). This can be expected as the ARCH process is a martingale. In the panel for $\zeta = 1$ we see that the uniform rejection frequencies are extremely close to unity for both the empirical curve and the $\log(n)$ -axis falling inside the confidence band (1.00 and 0.98, respectively). So normal tails and i.i.d.-ness are strongly rejected by the moment ratio curves based on absolute moments ($\zeta = 1$). Again we see that pointwise rejections are strongest for relatively low values of the return horizon n .

5 Application to foreign exchange data

In this section, we apply our hybrid volatility ratio test to the daily US/UK and the FF/DM spot exchange rates. The data were obtained from Datasream and span the period January 1986–December 1997. The number of observations is 3,129. The volatility ratio curves for the US/UK are presented in Figure 7.

First consider the $\zeta = 2$ plot for the US/UK series. The empirical curve rises slowly for small values of the return horizon n , and then levels off at larger return horizons. The curve remains well within the 95% confidence band. Furthermore, the $\log(n)$ -axis completely falls within the confidence interval. This signals that there is no significant linear dependence in this return series. Moreover, even if there is some (insignificant) correlation between returns, it appears not to be of the mean reverting type, cf. Figures 2 and 5. Also note that the average bootstrap variance ratio curve practically coincides with the $\log(n)$ -axis. The empirical evidence thus confirms the hypothesis that freely floating exchange rates are governed by a martingale.

The $\zeta = 1$ plot is also quite informative. The empirical moment ratio

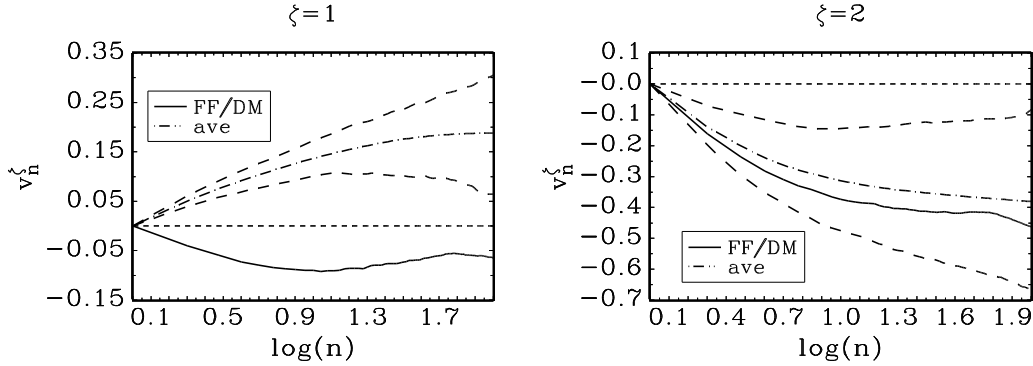


Figure 8: *Moment ratio curves for the FF/DM exchange rate from January 3, 1986 to December 31, 1997, with (block-)bootstrapped uniform confidence intervals.*

curve increases initially, and then levels off. The curve touches the edge of the 95 % confidence band, indicating that there may be some dependence in the second moments of the returns. The weak evidence for volatility clusters can be understood from the presence of Generalized ARCH effects in combination with heavy-tailed marginal innovations. Typical GARCH estimates give a dominant role to past volatility and only a moderate role to past (squared) exchange rate returns. This induces a moderate indication for ARCH when the marginal innovations are fat-tailed distributed, since the weak ARCH effect has only a moderate impact on lowering the curve for small n while the latter has a strong upward effect. The presence of fat-tailedness is clearly signalled by the fact that the confidence interval fails to cover a large part of the $\log(n)$ -axis. This non-normality is confirmed by the shape of the average bootstrap curve, which lies entirely above the $\log(n)$ -axis. Similar results were obtained for other freely floating currencies against the US dollar. In fact, for the dollar rates considered by Liu and He (1991) we never find evidence in favor of linear dependence. This contrasts with the conclusion of Liu and He and is due to the simultaneous consideration of the ratios at different horizons. For all these rates, however, we do find the heavy tail feature and weak ARCH effects; only in the Canadian/US dollar rate did we not find evidence for volatility clustering. Next we turn to non-freely floating rates.

Figure 8 presents the moment ratio curves for the FF/DM rate. Again we begin by considering the $\zeta = 2$ plot. The most striking feature is that the $\log(n)$ -axis lies completely above the confidence band. This implies that there is a high degree of first-order dependence in the returns. Thus, the martingale assumption is overwhelmingly rejected. The empirical curve, however, lies well within the confidence bands.

Turning to the $\zeta = 1$ case, we note that both the $\log(n)$ -axis and the empirical moment ratio curve lie entirely below the confidence band, while the average bootstrap curve rises above the $\log(n)$ -axis before levelling off somewhat at larger return horizons. The $\log(n)$ -axis and the empirical curve signal that there is significant linear dependence in the returns. The average bootstrap curve for $\zeta = 1$ reveals that the returns are fat-tailed because the confidence band is entirely above the x -axis.

An economic explanation for the FF/DM results is not hard to find. Because of the obligations arising from the ERM arrangement, the monetary authorities in France and Germany have frequently intervened since 1983 to keep the FF/DM rate within the predefined target zone. These interventions generate negative autocorrelation in the returns, see, e.g., Bertola (1994). This is exactly what we find in Figure 8. Similar pictures emerge for other managed (cross) rates.

6 Conclusions

The paper presents a new and generalized volatility ratio testing methodology. The statistic based on the ratio of the first absolute moments has not been considered before. Our methodology allows one to distinguish between first order linear dependence, fat-tailedness, and volatility clustering. The typical behavior of the moment ratios under these three types of deviations from the assumption of normal i.i.d. returns is obtained analytically. The approach is hybrid in the sense that we use a combination of formal statistical testing and pattern recognition based on graphical representations of moment ratios for various return horizons. The graphical representation provides a useful tool for exploratory data analysis and allows one to quickly assess the salient features of the data. The formal statistical inference procedure incorporated in the graphical representation heavily builds on the bootstrap. In contrast to previous research, this allows us to account for the correlation between moment ratio tests based on different return horizons without resorting to overly conservative confidence intervals.

We illustrated the methodology using simulations and empirical data. The simulated data allow one to build up an expert opinion in interpreting moment ratio curves. We particularly consider data generating processes that exhibit properties relevant in a (financial) economic context, e.g., fat-tailedness, linear dependence, and volatility clustering. We also consider the result of our testing procedure when applied to two spot exchange rate series. For the US/UK rate, we find no significant deviations from the martingale assumption. By contrast, there is a clear and significant indication of fat-

tailedness of the unconditional returns, which is due to fat-tailed conditional returns and some volatility clustering. For the FF/DM rate, we find significant negative autocorrelation, and again fat-tailed unconditional returns. The linear dependence accords with the substantial amount of intervention in this rate over the sample period.

References

- Abramowitz, M., and I.A. Stegun (1972): *Handbook of mathematical functions*. New York: Dover.
- Bertola, G. (1994): "Continuous-time models of exchange rates and intervention," in *The handbook of international macroeconomics*, ed. by F. van der Ploeg. Oxford: Blackwell.
- Campbell, J.Y., and N.G. Mankiw (1987): "Are output fluctuations transitory?" *Quarterly Journal of Economics*, **102**, 857-880.
- Campbell, J.Y., A.W. Lo, and A.C. MacKinlay (1997): *The econometrics of financial markets*. Princeton, NJ: Princeton University Press.
- Chow, K.V., and K.C. Denning (1993): "A simple multiple variance ratio test," *Journal of Econometrics*, **58**, 385-401.
- Cochrane, J.H. (1988): "How big is the random walk in GNP?" *Journal of Political Economy*, **96**, 893-920.
- Diebold, F.X. (1988): *Empirical modeling of exchange rate dynamics*. Berlin: Springer-Verlag.
- Ding, Z., C.W.J. Granger, and R.F. Engle (1993): "A long memory property of stock market returns and a new model," *Journal of Empirical Finance*, **1**, 83-106.
- Engle, R.F. (1982): "Autoregressive conditional heteroskedasticity with estimates of the variance of U.K. inflation," *Econometrica*, **50**, 987-1008.
- Fama, E.F., and K.R. French (1988): "Permanent and temporary components of stock prices," *Journal of Political Economy*, **96**, 246-273.
- Faust, J. (1992): "When are variance ratio tests for serial dependence optimal?" *Econometrica*, **60**, 1215-1226.
- Feller, W. (1971): *An introduction to probability theory and its applications*, vol. 2, 2nd edition. New York: John Wiley.

- Fong, W.M., S.K. Koh, and S. Ouliaris (1997): "Joint variance-ratio tests of the martingale hypothesis for exchange rates," *Journal of Business and Economic Statistics*, **15**, 51-59.
- Gradshteyn, I.S., and I.M. Ryzhik (1994): *Table of integrals, series, and products*, 5th edition. London: Academic Press.
- Granger, C.W.J., and Z. Ding (1995): "Some properties of absolute returns: An alternative measure of risk," *Annales d'Économie et de Statistique*, **40**, 67-91.
- Groenendijk, P.A., A. Lucas, and C.G. de Vries (1997): "Stochastic processes, non-normal innovations, and the use of scaling ratios," Research memorandum 1997-58, Free University Amsterdam.
- Guillaume, D.M., M.M. Dacorogna, R.R. Davé, U.A. Müller, R.B. Olsen, and O.V. Pictet (1997): "From the bird's eye to the microscope: A survey of new stylized facts of the intra-daily foreign exchange markets," *Finance and Stochastics*, **1**, 95-129.
- Haan, L. de, S.I. Resnick, H. Rootzén, and C.G. de Vries (1989): "Extremal behaviour of solutions to a stochastic difference equation with applications to ARCH processes," *Stochastic Processes and their Applications*, **32**, 213-224.
- Hall, P., J.L. Horowitz, and B.-Y. Jing (1995): "On blocking rules for the bootstrap with dependent data," *Biometrika*, **82**, 561-574.
- Hamilton, J.D. (1994): *Time series analysis*. Princeton, NJ: Princeton University Press.
- Huizinga, J.H. (1987): "An empirical investigation of the long-run behavior of real exchange rates," *Carnegie-Rochester Conference Series on Public Policy*, **27**, 149-214.
- Ibragimov, I.A., and Yu V. Linnik (1971): *Independent and stationary sequences of random variables*. Groningen: Wolters-Noordhoff.
- Liu, C.Y., and J. He (1991): "A variance-ratio test of random walks in foreign exchange rates," *Journal of Finance*, **46**, 773-785.
- Lo, A.W., and A.C. MacKinlay (1988): "Stock market prices do not follow random walks: Evidence from a simple specification test," *Review of Financial Studies*, **1**, 41-66.
- McCulloch, J.H. (1997): "Measuring tail thickness to estimate the stable index α : A critique," *Journal of Business and Economic Statistics*, **15**, 74-81.

- Müller, U.A., M.M. Dacorogna, R.B. Olsen, O.V. Pictet, M. Schwarz, and C. Morgeneegg (1990): “Statistical study of foreign exchange rates, empirical evidence of a price change scaling law, and intraday analysis,” *Journal of Banking and Finance*, **14**, 1189-1208.
- Nelson, D.B. (1990): “Stationarity and persistence in the GARCH(1,1) model,” *Econometric Theory*, **6**, 318-334.
- Pagan, A.R. (1996): “The econometrics of financial markets,” *Journal of Empirical Finance*, **3**, 15-102.
- Phillips, P.C.B. (1987): “Time series regression with a unit root,” *Econometrica*, **55**, 277-301.
- Poterba, J.M., and L.H. Summers (1988): “Mean reversion in stock prices: Evidence and implications,” *Journal of Financial Economics*, **22**, 27-59.
- Richardson, M. (1993): “Temporary components of stock prices: A skeptic’s view,” *Journal of Business and Economic Statistics*, **11**, 199-207.
- Richardson, M., and J.H. Stock (1989): “Drawing inferences from statistics based on multiyear asset returns,” *Journal of Financial Economics*, **25**, 323-348.
- Samorodnitsky, G., and M.S. Taqqu (1994): *Stable non-Gaussian random processes: Stochastic models with infinite variance*. New York: Chapman & Hall.
- Shao, J., and D. Tu (1995): *The jackknife and bootstrap*. New York: Springer Verlag.
- Taylor, S.J. (1986): *Modelling financial time series*. Chichester: John Wiley.

A Proof of Theorems

Proof of Theorem 1: First consider the case where $0 \leq \zeta < 2$. Following Ibragimov and Linnik (1971, Theorem 2.1.1),

$$\begin{aligned} \lim_{n \rightarrow \infty} \frac{\log \left(E \left(|r_t^n|^\zeta \right) \right)}{\log(n)} &= \lim_{n \rightarrow \infty} \left\{ \frac{\log \left((B_n)^\zeta \right)}{\log(n)} + \frac{\log \left(E \left(\left| \frac{r_t^n}{B_n} \right|^\zeta \right) \right)}{\log(n)} \right\} \\ &= \frac{\zeta}{\alpha} + \lim_{n \rightarrow \infty} \frac{E \left(\left| \frac{r_t^n}{B_n} \right|^\zeta \right)}{\log(n)}, \end{aligned}$$

where B_n is an appropriately chosen normalizing constant of the form $B_n = n^{1/\alpha} s(n)$, with $s(n)$ a slowly varying function, i.e., $\lim_{n \rightarrow \infty} s(tn)/s(n) = 1$ for $t > 0$. Using Ibragimov and Linnik (1971, Lemma 5.2.2), we have that

$$\frac{\zeta}{\alpha} + \lim_{n \rightarrow \infty} \frac{E \left(\left| \frac{r_t^n}{B_n} \right|^\zeta \right)}{\log(n)} \leq \frac{\zeta}{\alpha} + \lim_{n \rightarrow \infty} \frac{\Delta}{\log(n)} = \frac{\zeta}{\alpha},$$

where Δ is a positive constant that does not depend on n .

Next consider the case where $\zeta = \alpha = 2$. Note that

$$\begin{aligned} \lim_{n \rightarrow \infty} \frac{\log \left(E \left(|r_t^n|^2 \right) \right)}{\log(n)} &= \lim_{n \rightarrow \infty} \frac{\log \left(n E \left(|r_t^n/n^{1/2}|^2 \right) \right)}{\log(n)} \\ &= 1 + \lim_{n \rightarrow \infty} \frac{\log \left(E \left(|r_t^n/n^{1/2}|^2 \right) \right)}{\log(n)}. \end{aligned} \quad (\text{A.1})$$

It remains to be shown that the last term in (A.1) goes to zero as n tends to infinity. To prove this, note that

$$E \left(|r_t^n/n^{1/2}|^2 \right) = n^{-1} E \left(\left(\sum_{i=1}^n \varepsilon_i \right)^2 \right) = n^{-1} \sum_{i=1}^n E \left(\varepsilon_i^2 \right) = E \left(\varepsilon_i^2 \right),$$

which is finite by assumption. This establishes the theorem for $\zeta = \alpha = 2$, which completes the proof.

Proof of Theorem 2: Let the one-period returns $r_1^t = \varepsilon_t$ follow the distribution D , and let ξ_t be a standard normal random variate. By the Central Limit Theorem, we obtain

$$E \left(\left| n^{-1/2} r_t^n \right|^\zeta \right) \approx \left(E \left((\varepsilon_t)^2 \right) \right)^{\zeta/2} E \left(|\xi_t|^\zeta \right).$$

for sufficiently large n . Hence, $v_n^\zeta \geq 0$ is equivalent to (for sufficiently large n)

$$E \left(|\xi_t|^\zeta \right) \geq \frac{E \left(|\varepsilon_t|^\zeta \right)}{\left(E \left((\varepsilon_t)^2 \right) \right)^{\zeta/2}}. \quad (\text{A.2})$$

Note that for $\zeta = 2$, the LHS and RHS in (A.2) are equal to 1. But this need not be the case for $\zeta = 1$. For the normal law $E(|\varepsilon_t|)/\sqrt{E(\varepsilon_t^2)} = \sqrt{2/\pi}$.

Proof of Theorem 3: From Proposition (2.1) of Diebold (1988) we have that

$$\sqrt{\frac{1 - \sum_i \lambda_i}{n\omega}} \sum_{t=1}^n \varepsilon_t \rightarrow N(0, 1)$$

in distribution. Hence, as in the proof of the previous theorem, we can rewrite $v_n^\zeta \geq 0$ as

$$E(|\varepsilon_t|^\zeta) / E((\varepsilon_t)^2)^{\zeta/2} \leq \sqrt{2/\pi}, \quad (\text{A.3})$$

where $E((\varepsilon_t)^2) = \omega / (1 - \sum_i \lambda_i)$. It is immediate that for $\zeta = 2$, (A.3) is an equality. For $\zeta = 1$, the LHS of (A.3) can be written as

$$E(|\varepsilon_t|) / \sqrt{E((\varepsilon_t)^2)} = \sqrt{2/\pi} E(\sqrt{h_t}) / \sqrt{E(h_t)}.$$

Hence, (A.3) reduces to

$$E(\sqrt{H}) < \sqrt{E(H)},$$

which holds by Jensen's inequality.

Proof of Theorem 4: By assumption $E(x_t) = 0$, $E(x_t^2) = \sigma^2 < \infty$. From the definition (6)

$$V_2^1 = \frac{E(|\varepsilon_t + \varepsilon_{t-1}|)}{E(|\sqrt{2}\varepsilon_t|)}.$$

By substitution we have that

$$\varepsilon_{t-1} = x_{t-1} \sqrt{\omega + \lambda \varepsilon_{t-2}^2}, \quad \varepsilon_{t-1}|_{\lambda=0} = \sqrt{\omega} x_{t-1},$$

and

$$\varepsilon_t = x_t \sqrt{\omega (1 + \lambda x_{t-1}^2) + \lambda^2 x_{t-1}^2 \varepsilon_{t-2}^2}, \quad \varepsilon_t|_{\lambda=0} = \sqrt{\omega} x_t.$$

Partial differentiation of V_2^1 at $\lambda = 0$ with respect to λ yields

$$\begin{aligned} & \text{sign} \left\{ \frac{\partial V_2^1}{\partial \lambda} \Big|_{\lambda=0} \right\} \\ &= \text{sign} \left\{ \frac{\partial E(|\varepsilon_t + \varepsilon_{t-1}|)}{\partial \lambda} \Big|_{\lambda=0} E(|x_t|) - E(|x_t + x_{t-1}|) \frac{\partial E(|\varepsilon_t|)}{\partial \lambda} \Big|_{\lambda=0} \right\}. \end{aligned}$$

Let $K_{x_t}(\cdot)$ denote the distribution function of x_t , and let $F_{\varepsilon_{t-2}}$ be the unconditional distribution function of ε_{t-2} . By definition

$$\begin{aligned} E(|\varepsilon_t|) &= \int_{-\infty}^{\infty} \int_{-\infty}^{\infty} \int_0^{\infty} \varepsilon_t dK_{x_t} dK_{x_{t-1}} dF_{\varepsilon_{t-2}} \\ &\quad - \int_{-\infty}^{\infty} \int_{-\infty}^{\infty} \int_{-\infty}^0 \varepsilon_t dK_{x_t} dK_{x_{t-1}} dF_{\varepsilon_{t-2}}. \end{aligned}$$

Since

$$\left. \frac{\partial \varepsilon_t}{\partial \lambda} \right|_{\lambda=0} = \frac{1}{2} \sqrt{\omega} x_t x_{t-1}^2,$$

differentiation under the integral gives

$$\left. \frac{\partial E(|\varepsilon_t|)}{\partial \lambda} \right|_{\lambda=0} = \frac{1}{2} \sqrt{\omega} \sigma^2 E(|x_t|).$$

Hence,

$$\text{sign} \left\{ \left. \frac{\partial V_2^1}{\partial \lambda} \right|_{\lambda=0} \right\} = \text{sign} \left\{ \left. \frac{\partial E(|\varepsilon_t + \varepsilon_{t-1}|)}{\partial \lambda} \right|_{\lambda=0} - \frac{1}{2} \sqrt{\omega} \sigma^2 E(|x_t + x_{t-1}|) \right\}.$$

Similarly, for the convolution

$$\begin{aligned} E(|\varepsilon_t + \varepsilon_{t-1}|) &= \int_{-\infty}^{\infty} \int_{-\infty}^{\infty} \int_a^{\infty} (\varepsilon_t + \varepsilon_{t-1}) dK_{x_t} dK_{x_{t-1}} dF_{\varepsilon_{t-2}} \\ &\quad - \int_{-\infty}^{\infty} \int_{-\infty}^{\infty} \int_{-\infty}^a (\varepsilon_t + \varepsilon_{t-1}) dK_{x_t} dK_{x_{t-1}} dF_{\varepsilon_{t-2}}, \end{aligned}$$

with $a = -x_t \varepsilon_{t-1} / \varepsilon_t$. Note that at $\lambda = 0$: $a = -x_{t-1}$. The covariance stationarity of the process implies that $E(\varepsilon_{t-2}^2) = \omega \sigma^2 / (1 - \lambda \sigma^2)$, and hence at $\lambda = 0$: $E(\varepsilon_{t-2}^2) = \omega \sigma^2$. Also,

$$\left. \frac{\partial (\varepsilon_t + \varepsilon_{t-1})}{\partial \lambda} \right|_{\lambda=0} = \frac{1}{2} \sqrt{\omega} x_t x_{t-1}^2 + \frac{1}{2\sqrt{\omega}} x_{t-1} \varepsilon_{t-2}^2.$$

By Leibniz' rule we obtain

$$\begin{aligned} \left. \frac{\partial E(|\varepsilon_t + \varepsilon_{t-1}|)}{\partial \lambda} \right|_{\lambda=0} &= \int_{-\infty}^{\infty} \int_{-x_{t-1}}^{\infty} \left(\frac{1}{2} \sqrt{\omega} \sigma^2 x_{t-1} + \frac{1}{2} \sqrt{\omega} x_t x_{t-1}^2 \right) dK_{x_t} dK_{x_{t-1}} \\ &\quad - \int_{-\infty}^{\infty} \int_{-\infty}^{-x_{t-1}} \left(\frac{1}{2} \sqrt{\omega} \sigma^2 x_{t-1} + \frac{1}{2} \sqrt{\omega} x_t x_{t-1}^2 \right) dK_{x_t} dK_{x_{t-1}}. \end{aligned}$$

By definition,

$$\begin{aligned} E(|x_t + x_{t-1}|) &= \int_{-\infty}^{\infty} \int_{-x_{t-1}}^{\infty} (x_t + x_{t-1}) dK_{x_t} dK_{x_{t-1}} \\ &\quad - \int_{-\infty}^{\infty} \int_{-\infty}^{-x_{t-1}} (x_t + x_{t-1}) dK_{x_t} dK_{x_{t-1}}. \end{aligned}$$

Use these last two integral expressions to further simplify

$$\begin{aligned}
& \text{sign} \left\{ \frac{\partial V_2^1}{\partial \lambda} \Big|_{\lambda=0} \right\} = \\
& \text{sign} \left\{ \int_{-\infty}^{\infty} (x_{t-1}^2 - \sigma^2) \left(\int_{-x_{t-1}}^{\infty} x_t dK_{x_t} - \int_{-\infty}^{-x_{t-1}} x_t dK_{x_t} \right) dK_{x_{t-1}} \right\} = \\
& \text{sign} \left\{ -2 \int_{-\infty}^{\infty} (x_{t-1}^2 - \sigma^2) \int_{-\infty}^{-x_{t-1}} x_t dK_{x_t} dK_{x_{t-1}} \right\} = \\
& \text{sign} \left\{ \int_{-\infty}^{\infty} (x_{t-1}^2 - \sigma^2) A(x_{t-1}) dK_{x_{t-1}} \right\},
\end{aligned}$$

where $A(y) = -2 \int_{-\infty}^{-y} x dK_x$. The function $A(y)$ has the following two properties. Let $k_x(x)$ denote the density of the innovations x_t . The derivative of $A(y)$ is (by Leibniz' rule)

$$\frac{dA(y)}{dy} = -2yk(-y) \geq 0 \text{ as } y \leq 0.$$

Hence, $A(y)$ monotonically increases on $(-\infty, 0)$ and decreases on $(0, \infty)$. Furthermore $A(\infty) = A(-\infty) = 0$, $A(0) = E(|x|)$, and $A(y) \geq 0$. By the assumed symmetry of $k(x)$ it follows that $A(y)$ is symmetric around 0 as well. Hence, we can always find a constant $c > 0$ such that

$$cA(\sigma) = cA(-\sigma) = k(\sigma).$$

For this constant $cA(x) > 1$ on $[-\sigma, \sigma]$ and $cA(x) < 1$ for $x \notin [-\sigma, \sigma]$. Hence, $cA(x)k(x)$ has more mass in the center and less mass in the tails than $k(x)$. It is then immediate that

$$\text{sign} \left\{ \frac{\partial V_2^1}{\partial \lambda} \Big|_{\lambda=0} \right\} = \frac{1}{c} \text{sign} \left\{ \int_{-\infty}^{\infty} (x_{t-1}^2 - \sigma^2) cA(x_{t-1}) dK_{x_{t-1}} \right\} < 0.$$

Proof of Theorem 5: By Proposition 7.11 in Hamilton (1994),

$$\frac{1}{\sqrt{n}} \sum_{t=1}^n \varepsilon_t \rightarrow N \left(0, \sum_{j=-\infty}^{\infty} \gamma_j \right)$$

in distribution. Manipulating $v_n^{\zeta} \geq 0$ as before proves the theorem.

B Proofs of examples

B.1 Results for the Laplace distribution

The characteristic function of the standard Laplace distribution is

$$\int_{-\infty}^{\infty} \frac{1}{2} e^{isx} e^{-|x|} dx = \int_0^{\infty} \cos(sx) e^{-x} dx = \frac{1}{1+s^2},$$

see, e.g., Gradshteyn and Ryzhik (1994, p. 1191). Therefore, for Laplace distributed one-period returns, we obtain

$$E(\exp(isr_t^n)) = (E(\exp(is\varepsilon_t)))^n = \frac{1}{(1+s^2)^n}.$$

The density of r_t^n is given by the inverse Fourier transform of the characteristic function divided by $\sqrt{2\pi}$, i.e.,

$$\begin{aligned} f(r_t^n) &= \frac{1}{2\pi} \int_{-\infty}^{\infty} e^{-isr_t^n} (1+s^2)^{-n} ds = \frac{1}{\pi} \int_0^{\infty} \cos(sr_t^n) (1+s^2)^{-n} ds \\ &= \frac{1}{\sqrt{\pi}} \left(\frac{r_t^n}{2}\right)^{n-\frac{1}{2}} \frac{K_{n-\frac{1}{2}}(r_t^n)}{\Gamma(n)}, \end{aligned} \quad (\text{B.1})$$

with $f(r_t^n)$ denoting the density of r_t^n , and $K_\nu(\cdot)$ a Bessel function of the third kind for imaginary arguments (see Gradshteyn and Ryzhik (1994, pp. 961, 1191)). As the density of ε_t is symmetric around zero, so is the density of r_t^n . Therefore, the expectation of $|r_t^n|$ equals

$$E(|r_t^n|) = \int_{-\infty}^{\infty} |r_t^n| f(r_t^n) dr_t^n = 2 \int_0^{\infty} r_t^n f(r_t^n) dr_t^n. \quad (\text{B.2})$$

Using (B.1), (B.2) can be rewritten as

$$E(|r_t^n|) = \frac{1}{\sqrt{\pi}\Gamma(n)2^{n-\frac{3}{2}}} \int_0^{\infty} (r_t^n)^{n+\frac{1}{2}} K_{n-\frac{1}{2}}(r_t^n) dr_t^n. \quad (\text{B.3})$$

The integral in (B.3) can be recognized as the Mellin transform of $K_\nu(\cdot)$ with argument $n+3/2$ (see Gradshteyn and Ryzhik (1994, p. 1193)). Using the Mellin transform of $K_\nu(\cdot)$ as given in, e.g., Gradshteyn and Ryzhik (1994, p. 1195), (B.3) reduces to

$$E(|r_t^n|) = \frac{2}{\sqrt{\pi}} \cdot \frac{\Gamma(n+\frac{1}{2})}{\Gamma(n)}.$$

Using the result that $n^{-1/2}\Gamma(n+1/2)/\Gamma(n)$ tends to one as n tends to infinity (see Abramowitz and Stegun (1972, Equation 6.1.46)), it follows immediately that

$$\lim_{n \rightarrow \infty} \frac{\log(E(|r_t^n|)/E(|r_t^1|))}{\log(n)} = \frac{1}{2}.$$

B.2 Results for the Student- $t(3)$ distribution

Consider the Student- $t(3)$ distribution

$$t_3(x) = \frac{2}{\pi\sqrt{3}} \cdot \frac{1}{\left(1 + \frac{x^2}{3}\right)^2}.$$

The Fourier transform of the $t(3)$ distribution is given by (see Gradshteyn and Ryzhik (1994, p. 1191))

$$\frac{1}{\sqrt{2\pi}} \int_{-\infty}^{\infty} t_3(x) e^{itx} dx = \sqrt{\frac{2}{\pi}} \int_0^{\infty} \cos(tx) \cdot t_3(x) dx = \frac{(1 + \sqrt{3}|t|) e^{-\sqrt{3}|t|}}{\sqrt{2\pi}}.$$

The characteristic function is equal to $\sqrt{2\pi}$ times the Fourier transform, and is thus given by $(1 + \sqrt{3}|t|)e^{-\sqrt{3}|t|}$. Hence, the characteristic function of the n -period return is given by $(1 + \sqrt{3}|t|)^n e^{-n\sqrt{3}|t|}$. Therefore, the Fourier transform for the n -period return equals

$$\frac{(1 + \sqrt{3}|t|)^n e^{-n\sqrt{3}|t|}}{\sqrt{2\pi}}. \quad (\text{B.4})$$

The density of the n -period return r_t^n is given by the inverse Fourier transform of (B.4). Using this fact, $E(|r_t^n|)$ can be written as

$$\begin{aligned} E\left(\left|\sum_{i=1}^n \varepsilon_i\right|\right) &= \int_{-\infty}^{\infty} \frac{|x|}{\sqrt{2\pi}} \int_{-\infty}^{\infty} \frac{(1 + \sqrt{3}|t|)^n e^{-n\sqrt{3}|t|} e^{itx}}{\sqrt{2\pi}} dt dx \\ &= 2 \int_0^{\infty} x \sqrt{\frac{2}{\pi}} \int_0^{\infty} \frac{(1 + \sqrt{3}t)^n e^{-n\sqrt{3}t} \cos(tx)}{\sqrt{2\pi}} dt dx \\ &= 2 \int_0^{\infty} \frac{x}{\pi} \int_0^{\infty} \sum_{k=0}^{\infty} \binom{n}{k} (\sqrt{3}t)^k e^{-n\sqrt{3}t} \operatorname{Re}(e^{-itx}) dt dx \\ &= \frac{2}{\pi} \int_0^{\infty} \sum_{k=0}^n \binom{n}{k} x \operatorname{Re}\left(\int_0^{\infty} (\sqrt{3}t)^k \frac{e^{-t\sqrt{3}\left(n + \frac{ix}{\sqrt{3}}\right)}}{\sqrt{3}} dt \sqrt{3}\right) dx \\ &= \frac{2}{\pi} \int_0^{\infty} \sum_{k=0}^n \frac{n! 3^{-1/2}}{(n-k)!} \operatorname{Re}\left(\frac{x}{\left(n + \frac{ix}{\sqrt{3}}\right)^{k+1}}\right) dx, \end{aligned} \quad (\text{B.5})$$

where the last equality follows from Gradshteyn and Ryzhik (1994, p. 1178), and $\operatorname{Re}(x)$ denotes the real part of $x \in \mathbb{C}$, with \mathbb{C} the set of complex numbers. Note that integration and summation in (B.5) cannot be interchanged, as the individual terms in the integrals of the sum do not always exist. Therefore, we simplify (B.5) as follows. Note that (B.5) is equivalent to

$$\lim_{M \rightarrow \infty} \frac{2}{\pi} \sum_{k=0}^n \frac{n!}{(n-k)!} \sqrt{3} \operatorname{Re}\left(\int_0^M \frac{x}{(n+ix)^{k+1}} dx\right). \quad (\text{B.6})$$

Solving the integral in (B.6) yields

$$\int_0^M \frac{x}{(n+ix)^{k+1}} dx = \begin{cases} \frac{kiM+n}{k(k-1)(n+iM)^k} - \frac{1}{k(k-1)n^{k-1}}, & k \geq 2, \\ -iM + n \ln(n+iM) - n \ln(n), & k = 0, \\ \frac{iM}{n+iM} - \ln(n+iM) + \ln(n), & k = 1. \end{cases}$$

Substituting back this expression into (B.6), we obtain

$$\begin{aligned} & \lim_{M \rightarrow \infty} \frac{2\sqrt{3}}{\pi} \operatorname{Re} \left\{ -iM + n \ln(n+iM) - n \ln(n) + \frac{iMn}{n+iM} - n \ln(n+iM) \right. \\ & \quad \left. + n \ln(n) + \sum_{k=2}^n \frac{n!}{(n-k)!} \left\{ \frac{kiM+n}{k(k-1)(n+iM)^k} - \frac{1}{k(k-1)n^{k-1}} \right\} \right\} \\ &= \lim_{M \rightarrow \infty} \frac{2\sqrt{3}}{\pi} \operatorname{Re} \left\{ \frac{M^2}{n+iM} \right. \\ & \quad \left. + \sum_{k=2}^n \frac{n!}{(n-k)!} \left\{ \frac{ikM+n}{k(k-1)(n+iM)^k} - \frac{1}{k(k-1)n^{k-1}} \right\} \right\} \\ &= \lim_{M \rightarrow \infty} \frac{2\sqrt{3}}{\pi} \left\{ \frac{nM^2}{n^2+M^2} \right. \\ & \quad \left. + \sum_{k=2}^n \frac{n!}{(n-k)!} \left\{ \frac{ikM+n}{k(k-1)(n+iM)^k} - \frac{1}{k(k-1)n^{k-1}} \right\} \right\} \\ &= \frac{2\sqrt{3}}{\pi} \left\{ n - \sum_{k=2}^n \frac{n!}{(n-k)!k(k-1)n^{k-1}} \right\}. \end{aligned}$$

Hence

$$E \left(\left| \sum_{i=1}^n \varepsilon_i \right| \right) = \frac{2\sqrt{3}}{\pi} \left(n - (n-1) \sum_{k=0}^{n-2} \frac{(n-2)!}{(n-2-k)!(k+1)(k+2)n^k} \right).$$

Note that

$$\frac{1}{(k+1)(k+2)} = \frac{1}{k+1} - \frac{1}{k+2},$$

which implies

$$\begin{aligned} & \sum_{k=0}^{n-2} \frac{(n-2)!}{(n-2-k)!(k+1)(k+2)n^k} \\ &= 1 + \sum_{k=0}^{n-3} \frac{(n-2)!}{(n-3-k)!n^{k+1}(k+2)} - \sum_{k=0}^{n-3} \frac{(n-2)!}{(n-2-k)!n^k(k+2)} - \frac{(n-2)!}{n^{n-1}} \\ &= 1 - \frac{(n-2)!}{n^{n-1}} - \sum_{k=0}^{n-3} \frac{(n-2)!}{(n-2-k)!n^{k+1}}. \end{aligned}$$

From Stirling's formula (see Abramowitz and Stegun (1972, p. 257)), it follows that $(n-2)!/n^{n-1}$ is exponentially small for large n . Next, we prove

$$\sum_{k=0}^{n-3} \frac{(n-2)!}{(n-2-k)!n^k} = c \cdot \sqrt{n} + o(\sqrt{n}), \quad (\text{B.7})$$

for some constant $c > 0$, where $o(\sqrt{n})$ denotes a function that has an order of magnitude smaller than \sqrt{n} for large n .

Using Stirling's formula, i.e.,

$$n! = \sqrt{2\pi n} n^n \exp\left(-n + \frac{\theta}{n}\right),$$

where $0 < \theta < 1/12$, we obtain

$$\begin{aligned} \sum_{k=0}^{n-3} \frac{(n-2)!}{(n-2-k)!n^k} &= \left(\sum_{k=0}^{n-2} \frac{(n-2)!}{(n-2-k)!n^k} \right) - \frac{(n-2)!}{n^{n-2}} \\ &= \frac{(n-2)!}{n^{n-2}} \sum_{k=0}^{n-2} \frac{n^k}{k!} + o(\sqrt{n}) \\ &= \sqrt{2\pi} \left(1 - \frac{2}{n}\right)^{n-2} e^{\frac{\theta}{n-2}} \sqrt{n-2} e^{-n+2} \sum_{k=0}^{n-2} \frac{n^k}{k!} + o(\sqrt{n}). \end{aligned}$$

As $n \rightarrow \infty$,

$$\sqrt{2\pi} \left(1 - \frac{2}{n}\right)^{n-2} e^{\frac{\theta}{n-2}+2} \longrightarrow \sqrt{2\pi}.$$

It now remains to be proved that

$$\lim_{n \rightarrow \infty} \frac{\sum_{k=0}^{n-2} \frac{n^k}{k!}}{e^n} > 0.$$

Let \bar{P}_λ denote a Poisson distributed random variable with mean λ . Then

$$\begin{aligned} \sum_{k=0}^n \frac{e^{-n} n^k}{k!} &= P(\bar{P}_n \leq n) \\ &= P\left(\sum_{i=1}^n (\bar{P}_1^{(i)} - 1) / \sqrt{n} \leq 0\right) \\ &\longrightarrow \frac{1}{2} \end{aligned}$$

according to the standard central limit theorem, with $\{\bar{P}_1^{(i)}\}_{i=1}^n$ a set of i.i.d. Poisson distributed random variables with mean 1. This completes the proof of (B.7). It now follows directly from (B.7) that

$$\lim_{n \rightarrow \infty} \frac{\log(E(|r_t^n|)/E(|r_t^1|))}{\log(n)} = \frac{1}{2}.$$

B.3 Results for the Bernoulli distribution

Consider ε_t following the shifted Bernoulli as explained in example 1. Since $r_t^n \equiv \sum_{i=0}^{n-1} \varepsilon_{t-i}$, it follows that $r_t^n + n/2$ has a binomial distribution with parameters $(n, 1/2)$. For even and odd values of n , the expectation of the absolute moment can be derived as

$$E(|r_t^n|) = 2 \sum_{k=0}^{\frac{n}{2}-1} \binom{n}{k} \left(\frac{1}{2}\right)^n \left(\frac{n}{2} - k\right) = \frac{2^{-n} n!}{\left(\frac{n}{2}\right)! \left(\frac{n}{2} - 1\right)!}, \quad (\text{B.8})$$

and

$$E(|r_t^n|) = 2 \sum_{k=0}^{\frac{n-1}{2}} \binom{n}{k} \left(\frac{1}{2}\right)^n \left(\frac{n}{2} - k\right) = \frac{2^{-n} n!}{\left(\frac{n}{2} - \frac{1}{2}\right)! \left(\frac{n}{2} - \frac{1}{2}\right)!}, \quad (\text{B.9})$$

respectively. We now have that

$$E(|r_t^n|) = \frac{2^{-n} n!}{\left[\frac{n}{2}\right]! \left[\frac{n-1}{2}\right]!},$$

where $[X]$ is the integer part of X . Applying Stirling's formula (see Abramowitz and Stegun (1972, p. 257)) to (B.8) and (B.9) respectively, we obtain

$$E(|r_t^n|) = \frac{2^{-n} \sqrt{2\pi} n^n \sqrt{n} \exp\left(-n + \frac{\vartheta_1}{n}\right)}{2\pi (n-1)^{n-1} 2^{-n}(n-1) \exp\left(-n + 1 + \frac{2\vartheta_2}{n}\right)} \sim \sqrt{n},$$

and

$$E(|r_t^n|) = \frac{2^{-n-1} \sqrt{2\pi} n^{n+1} \sqrt{n} \exp\left(-n + \frac{\vartheta_1}{n}\right)}{2\pi n^n 2^{-n-1} n \exp\left(-n + \frac{2\vartheta_3}{n}\right)} \sim \sqrt{n},$$

for n is even and odd, respectively.

B.4 Results for ARMA(1,1) log prices

Rewriting (10) using backward substitution, we obtain

$$p_t = \varphi^t p_0 + \varepsilon_t - \theta \varphi^{t-1} \varepsilon_0 + (\varphi - \theta) \sum_{i=0}^{t-2} \varphi^i \varepsilon_{t-1-i}.$$

This implies that for $t \geq 1$,

$$\begin{aligned} E\left((p_t - p_0)^2\right) &= (\varphi^t - 1)^2 E(p_0^2) + 1 + \theta^2 \varphi^{2t-2} - 2\theta \varphi^{t-1} (\varphi^t - 1) \\ &\quad + \frac{(\varphi - \theta)^2 (1 - \varphi^{2t-2})}{1 - \varphi^2} \\ &= \frac{(\varphi^t - 1)(1 - 2\theta\varphi + \theta^2)}{1 - \varphi^2} + 1 + \theta^2 \varphi^{2t-2} - 2\theta \varphi^{t-1} (\varphi^t - 1) \\ &\quad + \frac{(\varphi - \theta)^2 (1 - \varphi^{2t-2})}{1 - \varphi^2} \\ &= \frac{2(1 - \varphi^t)(1 - 2\theta\varphi + \theta^2)}{1 - \varphi^2} + 2\theta \varphi^{t-1}. \end{aligned}$$

The result now follows from the stationarity of r_t^n and the observation that $r_0^t = p_t - p_0$.